NASA Contractor Report 177926

INTERACTION OF PART-THROUGH CRACKS IN A FLAT PLATE

B. Aksel and F. Erdogan

LEHIGH UNIVERSITY
Bethlehem, Pennsylvania

Grant NGR 39-007-011
April 1985

National Aeronautics and
Space Administration

Langley Research Center
Hampton, Virginia 23665

ABSTRACT

Main purpose of this study is to determine the accuracy of the line spring model, to investigate the effect of interaction between two and three cracks, and to provide extensive numerical results which may be useful in applications. Line spring model with Reissner's plate theory is formulated to be used for any number and configurations of cracks provided that there is symmetry. This model is used to find stress intensity factors for elliptic internal cracks, elliptic edge cracks and two opposite elliptic edge cracks. Unfortunately, because of the unavailability of previous work done on the cases considered, only stress intensity factors for central elliptic crack could be compared with other methods. Despite the simplicity of the line spring model, the results are found to be surprisingly close.

1. INTRODUCTION

From the viewpoint of practical applications, the analysis of a part through crack in a structural component which may locally be represented by a "plate" or a "shell" is certainly one of the most important problems in fracture mechanics. In its general form, the problem is a three-dimensional crack problem in a bounded geometry where the stress fields perturbed by the crack interacts very strongly with the surfaces of the solid. At present, even for the linearly elastic solids, a neat analytical treatment of the problem very heavily rely on some kind of numerical technique, such as alternating method, [5], [6], or boundary integral equation method, [7]; but most notably on the finite element method, [8]-[10]. The renewed interest in recent years in the so called "line-spring model" first described in [3] has been due partly to the desire of providing simpler and less expensive solutions to the part-through crack problem and partly to the fact that for certain important crack geometries, the model seems to give results that have an acceptable degree of accuracy.

In a plate or shell containing a part-through crack and subjected to membrane and bending loads, the net ligament(s) around the crack would generally have a constraining effect on the crack surface displacements and rotations. The basic idea underlying the "line-spring model" consists of approximating the three-dimensional

crack problem by a two-dimensional coupled bending-membrane problem through the reduction of the net ligament stresses to the neutral surface of the plate or shell as a membrane load N and a bending moment M. In the resulting two-dimensional problem, the crack surface displacements are represented by a crack opening displacement δ and a crack surface rotation θ, referred to, again, the neutral surface. The quantities N, M, δ and θ are assumed to be functions of a single variable, namely the coordinate x_1, along the crack in the neutral surface (Fig. 1). The pair of functions (δ,θ) or (N,M) are determined from the corresponding mixed boundary value problem for the plate or the shell having a through crack in which N and M are treated as unknown crack surface loads. Once N and M are determined, the stress intensity factors are evaluated from the two-dimensional elasticity solution of a strip under the membrane force N and the bending moment M.

The model introduced in [3] is based on the classical theory. However, the asymptotic stress field around the crack tip given by classical plate bending theory is not consistant with the elasticity solutions, whereas a transverse shear theory (such as that of Reissner's) which can accomodate all stress and moment resultants on the crack surface seperately (i.e., three boundary conditions in plates, five in shells) give results which are identical to the asymptotic solutions obtained from the plane strain and anti-plane shear crack problems [2], [11]. The line spring model was later used

in [12], [13] to treat the longitudinal part-through crack problem in a cylinder by using the classical shell theory and in [1], [14] by using transverse shear theory. Rather extensive results for corner cracks and for collinear surface cracks in a plate having a finite width are given in [15]. The similar problem of surface crack-boundary interaction in a cylindrical shell with a free or a fixed boundary is considered in [16] and [17].

In this study, stress intensity factors for elliptic internal cracks under pure bending and tension, and for collinear elliptic edge cracks under pure tension will be studied by using the line-spring model with Reissner's plate bending theory. Interaction of two and three identical elliptic edge and internal crcaks will also be studied by using the same method.

2. FORMULATION OF THE PROBLEM

2.1 Governing Integral Equations

The problem under consideration is a surface or an internal crack problem for a relatively thin-walled structural component which is solved basically as a plate or shell problem. In the usual notation u_1, u_2, u_3 are the components of the displacement vector, β_1 and β_2 are the angles of rotation of the normal to the neutral surface in x_1x_3 and x_2x_3 planes, respectively, and N_{ij}, M_{ij} and $V_i(i,j=1,2)$ are respectively the membrane, moment and transverse shear resultants (Fig. 1).

Related mixed boundary value problem for any number of cracks has been formulated in [15] by using Reissner's plate bending theory. The derivatives of the crack surface displacement and the crack surface rotation on the neutral surface are chosen as the unknown functions. Fredholm kernels $k_1(x,t)$ and $k_2(x,t)$ in [15] represent the effect of finite length of the plate in x_1 direction. They will vanish in this case since the plate has an infinite length in x_1 direction. Integral equations are written for only half of the infinite plate ($x_1 > 0$) and are only valid when symmetry with respect to the x_2x_3 plane exists. D represents the normalized cracked region on the x_1 axis, which means that if there is a crack in the region (b,c), D represents the region (b/a , c/a) where "a"

is the half crack length and equals to (c-b)/2. x is also normalized parameter on x_1 axis which is $x=x_1/a_i$, where a_i the half crack length for the corresponding crack(i subscript is needed because general formulation is done for more than one crack).

From [15], integral equations are as follows:

$$\frac{\sigma(x)}{E} - \frac{1}{2\pi}\int_D \left[\frac{1}{t-x} + \frac{1}{t+x}\right] G_1(t)\,dt = \frac{\sigma_o(x)}{E}, \qquad x \in D\,, \qquad (1)$$

$$\frac{m(x)}{6E} - R_1\int_D \left[R_2\left[\frac{1}{t-x} + \frac{1}{t+x}\right] - R_3\left[\frac{1}{(t-x)^3} + \frac{1}{(t+x)^3}\right] + R_4\left[\frac{1}{t-x}K_2(p|t-x|) + \frac{1}{t+x}K_2(p|t+x|)\right]\right] G_2(t)\,dt = \frac{m_o(x)}{6E}\,, \qquad x \in D\,, \qquad (2)$$

where K_2 is the modified Bessel function of the second kind and the constants R_1, R_2, R_3, R_4 and p are defined in Appendix I. h is the thickness of the plate, 2a is the length and $L(x_1)$ is the depth of the crack (Fig. 1). E is the modulus of elasticity and ν is the Poisson's ratio of the material. The unknown functions are defined by

$$G_1(x) = \frac{\partial}{\partial x} \mathfrak{F}_y(x,+0) , \qquad G_2(x) = \frac{\partial}{\partial x} v(x,+0) , \qquad (3)$$

$$\mathfrak{F}_y = \mathfrak{F}_2 , \qquad v = u_2/a .$$

The external loads

$$\sigma_o = \frac{N_{22}^o}{h} , \qquad m_o = \frac{6M_{22}^o}{h^2} , \qquad (4)$$

represent uniform membrane and bending resultants applied to the plate away from the crack region and σ and m which are defined by

$$\sigma(x) = \frac{N(x,0)}{h} , \qquad m(x) = \frac{6M(x,0)}{h^2} , \qquad x \in D , \qquad (5)$$

are the membrane and bending loads applied to the crack surfaces (Fig. 1). The integral equations are obtained from the following mixed boundary conditions in $x_2=0$ plane

$$N_{22}(x,0) = -N_{22}^{o} + N(x) \quad , \quad x \in D \ , \qquad (6a)$$

$$u_2(x,0) = 0 \quad , \quad x \in D \ , \qquad (6b)$$

$$M_{22}(x,0) = -M_{22}^{o} + M(x) \quad , \quad x \in D \ , \qquad (7a)$$

$$\beta_2(x,0) = 0 \quad , \quad x \in D \ , \qquad (7b)$$

where the general principle of superposition is used to account for the loading N_{22}^{o}, and M_{22}^{o} applied to the structure away from the crack region.

2.2 Line-Spring Model for an Edge Crack

Edge crack is chosen for introductory purposes because of the simplicity of its formulation. Modifications will be made as more complicated crack geometries are examined.

The configuration studied here is an "infinite" elastic plate of thickness h, which contains a surface crack of length 2a and depth $L(x_1)$ penetrating part through the thickness (Fig. 1). For general purposes $L(x_1)$can be any function which enables us to treat any crack geometry. At remote distances from the crack site, the plate is subjected to loads equipollent to a uniform simple tension in the x_2 direction and to pure bending about the x_1 axis. The first

assumption in the line-spring analysis is that the stress intensity factor at a point along the crack front with coordinate x_1 is identical to the stress intensity factor for an edge cracked strip in plane strain (Fig. 2), subjected to an axial force and moment equal, respectively, to $N_{22}(x_1,0)$ and $M_{22}(x_1,0)$, and having a crack depth equal to $L(x_1)$. In [1], [3], mode I stress intensity factor for the plane strain problem is given as

$$K(s) = \sqrt{h}\,[\sigma g_t(s) + m g_b(s)] \,, \qquad (8)$$

$$s(x_1) = L(x_1)/h \,, \qquad (9)$$

where functions $g_t(s)$ and $g_b(s)$ are called shape functions for tension and bending respectively, and given as

$$g_t(s) = \sqrt{\pi s}\sum_{i=1}^{n} b_i s^{2(i-1)} \,, \qquad (10a)$$

$$g_b(s) = \sqrt{\pi s}\sum_{i=1}^{n} c_i s^{(i-1)} \,. \qquad (10b)$$

The value of n is chosen according to the desired accuracy. The coefficients b_i and c_i can be found by a suitable curve fitting (Appendix II). Coefficients of the shape functions for a number of crack geometries are given in Tables 2, 4, 6, 8, 10, 12, 14, 16, 17.

In order to obtain $N(x_1)$ and $M(x_1)$ in terms of G_1 and G_2, the energy available for fracture along the crack front is expressed in two different ways, namely as the crack closure energy and as the product of load-load point displacement. In a plate with an edge crack subjected to uniform tension N and uniform bending moment M (Fig. 2), if K is the stress intensity factor given by the plane strain solution, from the crack closure energy, the energy (per unit width) available for fracture may be obtained as

$$G = \frac{\partial}{\partial L}(U-V) = \frac{1-\nu^2}{E} K^2 \quad , \tag{11}$$

where U is the work done by the external loads and V is the strain energy.

Let δ and θ be the load line displacements corresponding to N and M shown in Fig. 2 and $d\delta$ and $d\theta$ be the changes in δ and θ as the crack length goes from L to L+dL under fixed load conditions. Then referring to Fig. 2, the changes in U and V may be expressed as

$$dU = N d\delta + M d\theta \quad , \tag{12}$$

$$dV = (1/2)\,[N(\delta+d\delta) + M(\theta+d\theta) - (1/2)\,(N\delta + M\theta) =$$

$$= (1/2)\,(N d\delta + M d\theta) \quad , \tag{13}$$

Equations (12) and (13) give the energy available for a crack growth dL as follows:

$$d(U-V) = (1/2)\,(N d\delta + M d\theta) \quad . \tag{14}$$

On the other hand for constant N and M, and for a change of dL in the crack length, we have

$$d\delta = \frac{\partial \delta}{\partial L} dL \,, \qquad d\theta = \frac{\partial \theta}{\partial L} dL \quad . \tag{15}$$

Thus, from (14) and (15) it follows that

$$\frac{\partial}{\partial L}(U-V) = G = \frac{1}{2}\left[N\frac{\partial \delta}{\partial L} + M\frac{\partial \theta}{\partial L}\right], \tag{16}$$

and, by using (11) we find

$$\frac{1}{2}\left[N\frac{\partial \delta}{\partial L} + M\frac{\partial \theta}{\partial L}\right] = \frac{1-\nu^2}{E} K^2 \quad . \tag{17}$$

From (5) and (8), we may rewrite (17) in terms of σ and m as

follows:

$$\frac{1}{2}\left[\sigma h\frac{\partial\delta}{\partial L}+\frac{m}{6}\frac{h^2\partial\theta}{\partial L}\right]=h\frac{1-\nu^2}{E}(g_t^2\sigma^2+2g_tg_b\sigma m+g_b^2m^2)\ . \qquad (18)$$

In order to solve σ and m in terms of δ and θ or vice versa we introduce the so called compliance coefficients. In a cracked strip, displacement and rotation are functions of both the applied stress and bending moment. This relation may be expressed as

$$h\delta = A_{tt}\sigma + A_{tb}m\ , \qquad (19a)$$

$$h^2\theta/6 = A_{bt}\sigma + A_{bb}m\ , \qquad (19b)$$

where (with proper normalizations) $A_{tb}=A_{bt}$ by elastic reciprocity. The compliance coefficients A_{ij} depend only on L and vanish when L=0. If we substitute (19) into (18) and equate common coefficients in the quadratic forms of both sides, we get

$$\frac{dA_{tt}}{dL}=\frac{2(1-\nu^2)h}{E}g_t^2\ , \qquad (20a)$$

$$\frac{dA_{tb}}{dL} = \frac{dA_{bt}}{dL} = \frac{2(1-\nu^2)h}{E} g_t g_b \ , \qquad (20b)$$

$$\frac{dA_{bb}}{dL} = \frac{2(1-\nu^2)h}{E} g_b^2 \ . \qquad (20c)$$

By defining

$$\alpha_{ij} = h^{-1} \int_0^L g_i g_j \, dL \ , \quad (i,j = b,t) \ , \qquad (21)$$

and knowing that $A_{ij}=0$ at $L=0$, we may write

$$A_{tt} = \frac{2h^2(1-\nu^2)}{E} \alpha_{tt} \ , \qquad (22a)$$

$$A_{tb} = A_{bt} = \frac{2h^2(1-\nu^2)}{E} \alpha_{tb} \ , \qquad (22b)$$

$$A_{bb} = \frac{2h^2(1-\nu^2)}{E} \alpha_{bb} \ . \qquad (22c)$$

Substitution of (22) into (19) gives

$$\delta = \frac{2h(1-\nu^2)}{E} (\alpha_{tt}\sigma + \alpha_{tb}m) , \tag{23}$$

$$\theta = \frac{12(1-\nu^2)}{E} (\alpha_{bt}\sigma + \alpha_{bb}m) , \tag{24}$$

where $\alpha_{tb}=\alpha_{bt}$. From (3), δ and θ may be expressed in terms of the unknown functions G_1 and G_2 as

$$\theta = 2\beta_2(x,+0) = 2\int_{-1}^{x} G_1(t)\,dt , \tag{25}$$

$$\delta = 2au_2(x,+0) = 2a\int_{-1}^{x} G_2(t)\,dt . \tag{26}$$

If we solve (23) and (24) for $\sigma(x)$ and $m(x)$ and substitute (25) and (26) for δ and θ, we can determine $\sigma(x)$ and $m(x)$ in terms of the unknown functions G_1 and G_2 as follows:

$$\sigma(x) = E\left[\gamma_{tt}(x)\int_{-1}^{x} G_2(t)\,dt + \gamma_{tb}(x)\int_{-1}^{x} G_1(t)\,dt\right] , \tag{27}$$

$$m(x) = 6E \left[\gamma_{bt}(x) \int_{-l}^{x} G_2(t)\, dt + \gamma_{bb}(x) \int_{-l}^{x} G_1(t)\, dt \right] , \quad (28)$$

where

$$\gamma_{tt} = \frac{a}{h(1-\nu^2)} \frac{\alpha_{bb}}{\Delta} , \quad (29a)$$

$$\gamma_{tb} = -\frac{1}{6(1-\nu^2)} \frac{\alpha_{tb}}{\Delta} , \quad (29b)$$

$$\gamma_{bt} = -\frac{1}{6h(1-\nu^2)} \frac{\alpha_{bt}}{\Delta} , \quad (29c)$$

$$\gamma_{bb} = \frac{1}{36(1-\nu^2)} \frac{\alpha_{tt}}{\Delta} , \quad (29d)$$

$$\Delta = \alpha_{tt}\alpha_{bb} - \alpha_{tb}^2 . \quad (29e)$$

We should keep in mind that α_{ij} is a function of L(x)/h, which means α_{ij} is also a function of x.

For a single crack shown in Fig. 1, the normalized cracked region on x_1 axis (called D in (1) and (2)) is defined as (0,1). (1) and (2) then become

$$\frac{\sigma(x)}{E} - \frac{1}{2\pi}\int_0^1 \left[\frac{1}{t-x} + \frac{1}{t+x}\right] G_1(t)\, dt = \frac{\sigma_o}{E}, \quad 0 < x < 1, \tag{30}$$

$$\frac{m(x)}{6E} - R_1 \int_0^1 \left[R_2 \left(\frac{1}{t-x} + \frac{1}{t+x} \right) - R_3 \left[\frac{1}{(t-x)^3} + \frac{1}{(t+x)^3} \right] + R_4 \left[\frac{1}{t-x} K_2(p|t-x|) + \frac{1}{t+x} K_2(p|t+x|) \right] \right] G_2(t)\, dt$$

$$= \frac{m_o}{6E}, \qquad 0 < x < 1. \tag{31}$$

For convenience in the numerical solution of integral equations we need to convert the integrals calculated over (0,1) to (-1,1). Because of that the geometry and loading conditions are symmetric with respect to the x_2x_3 plane, $u_2(x,+0)$ and $\beta_2(x,+0)$ should also be symmetric with respect to the same plane. In mathemathical form

$$u_2(-x,+0) = u_2(x,+0), \tag{32a}$$

$$\beta_2(-x,+0) = \beta_2(x,+0) \ . \qquad (32b)$$

Observing that derivative of a symmetric function is antisymmetric, we may write

$$G_1(-t) = -G_1(t) \ , \qquad (33a)$$

$$G_2(-t) = -G_2(t) \ . \qquad (33b)$$

By applying the above properties, integrand of (30) can be rewritten as

$$\int_0^1 \left[\frac{1}{t-x} + \frac{1}{t+x}\right] G_1(t)\, dt = \int_0^1 \frac{1}{t-x} G_1(t)\, dt + \int_0^1 \frac{1}{t_1+x} G_1(t_1)\, dt_1 \ . \qquad (34)$$

By a change of variable $t_1 = -t$ and from (33a), we can write

$$\int_0^1 \frac{1}{t_1+x}\, G_1(t_1)\, dt_1 = \int_0^{-1} \frac{1}{-t+x}\, [-G_1(t)]\, (-dt)$$

$$= \int_{-1}^{0} \frac{1}{t-x}\, G_1(t)\, dt \quad . \qquad (35)$$

Substituting (35) in (34)

$$\int_0^1 \left[\frac{1}{t-x} + \frac{1}{t+x}\right] G_1(t)\, dt = \int_{-1}^{1} \frac{1}{t-x}\, G_1(t)\, dt \quad . \qquad (36)$$

After applying the same procedure to (31) and substituting (27) and (28) for $\sigma(x)$ and $m(x)$, integral equations take the following final form

$$\gamma_{bb}(x) \int_{-1}^{x} G_1(t)\, dt - R_1 \int_{-1}^{1} \left[R_2 \frac{1}{t-x} - R_3 \frac{1}{(t-x)^3}\right.$$

$$\left. + R_4 \frac{1}{t-x} K_2(p|t-x|)\right] G_1(t)\, dt + \gamma_{bt}(x) \int_{-1}^{x} G_2(t)\, dt$$

$$= \frac{m_o}{6E} \quad , \quad -1 < x < 1 \quad , \qquad (37a)$$

$$\Psi_{tb}(x)\int_{-1}^{x} G_1(t)\,dt + \Psi_{tt}(x)\int_{-1}^{x} G_2(t)\,dt - \frac{1}{2\pi}\int_{-1}^{1}\frac{G_2(t)}{t-x}dt = \frac{\sigma_o}{E}\,, \quad -1 < x < 1\,. \tag{37b}$$

From (3) it follows that the unknown functions G_1 and G_2 must satisfy the single valuedness conditions given by

$$\int_{-1}^{1} G_1(t)\,dt = 0\,, \qquad \int_{-1}^{1} G_2(t)\,dt = 0\,. \tag{38}$$

After solving (37) and (38) by using Gauss-Chebyshev closed type integration formula which is defined in Appendix III, a backward procedure is applied to find the stress intensity factors along the crack front. Unknown functions are integrated (Appendix IV) from -1 to the value of x at which the stress intensity factor is desired. Then those integrals are substituted to (27) and (28) with the functions $\Psi_{ij}(x)$, (i,j=t,b) evaluated at that particular point to get corresponding σ and m. Once σ and m are found, (8) gives the stress intensity factor at a specific point on the crack front.

2.3 Internal Cracks

The line-spring model described in the previous section may easily be extended to internal cracks such as that shown in Fig. 3. In this case the basic integral equations remain the same and again are given by (1) and (2). However, there are two crack tips (shown as A and B in Fig. 3) which create two different stress intensity factors for each cross-section taken perpendicular to x_1 direction. Previous assumptions regarding the stress intensity factors will also remain the same; however, they are now defined seperately, i.e.,

$$K_A = \sqrt{h}\,[\sigma g_{At}(s) + m g_{Ab}(s)] \quad , \qquad (39a)$$

$$K_B = \sqrt{h}\,[\sigma g_{Bt}(s) + m g_{Bb}(s)] \quad , \qquad (39b)$$

where g_{At}, g_{Ab}, g_{Bt}, g_{Bb} are the shape functions corresponding to crack tips A and B. Unlike the edge crack case, these shape functions are now functions of both $L(x_1)/h$ and d/h where d is the distance from the center of the crack to the neutral plane. Two way

parametrization is needed in order to define the shape functions which are valid for any kind of internal crack. Since elliptic cracks whose major axis are parallel to the free surface are the main concern in the present study, parametrization can be simplified by observing that the distance between the center of any crack obtained by taking cross-sections perpendicular to the major axis and the center line of the plate is fixed. In other words, d is constant for any elliptic crack whose major axis is parallel to the free surface. Because of this property, as in the previous case, we may again define the shape functions for each crack as a function of only one variable, which is $L(x_1)/h$, as

$$g_{At} = \sqrt{\pi s} \sum_{i=1}^{n} b_{Ai} s^{2(i-1)} \quad , \qquad (40a)$$

$$g_{Ab} = \sqrt{\pi s} \sum_{i=1}^{n} c_{Ai} s^{i-1} \quad , \qquad (40b)$$

$$g_{Bt} = \sqrt{\pi s} \sum_{i=1}^{n} b_{Bi} s^{2(i-1)} \quad , \qquad (40c)$$

$$g_{Bb} = \sqrt{\pi s} \sum_{i=1}^{n} c_{Bi} s^{i-1} \quad . \qquad (40d)$$

Keep in mind that coefficients are different for each value of d.

The next step is the representation of the energy available for fracture in terms of both stress intensity factors and product of load-load point displacement. As L increases by dL, the energy

increment available for fracture may be expressed as

$$d(U-V) = \frac{1-\nu^2}{E}\left[K_A^2\, d(L/2) + K_B^2\, d(L/2)\right] \quad , \tag{41}$$

giving

$$G = \frac{\partial}{\partial L}(U-V) = \frac{1-\nu^2}{2E}(K_A^2 + K_B^2) \quad , \tag{42}$$

which replaces (11). The rate of energy available for fracture as expressed in terms of the load line displacements and forces remains the same and is given by (16). If the same procedure as in the previous section is followed, the functions $\alpha(ij)$ may be found as

$$\alpha_{tt} = h^{-1} \int_0^L (g_{At}^2 + g_{Bt}^2)/2 \, dL \quad , \tag{43a}$$

$$\alpha_{bb} = h^{-1} \int_0^L (g_{Ab}^2 + g_{Bb}^2)/2 \, dL \quad , \tag{43b}$$

$$\alpha_{tb} = \alpha_{bt} = h^{-1} \int_0^L (g_{At}g_{Ab} + g_{Bt}g_{Bb})/2 \, dL \quad . \tag{43c}$$

After this point, everything, including the resulting integral

equations and the solution method, is exactly the same as explained in Section 2.2. After solving the equations, the functions G_1 and G_2 are again substituted to (27) and (28) to find σ and m, which are then substituted to (39) to find the two stress intensity factors at the corresponding value of x.

2.4 Symmetric Internal Crack

This is a special case of an internal crack where d=0. Due to the fact that simple tension cannot create any crack surface rotation and simple bending cannot create any crack opening displacement (on the neutral plane), from (23) and (24) one can write

$$\alpha_{tb} = \alpha_{bt} = 0 \quad , \qquad (44)$$

which gives

$$\gamma_{tb} = \gamma_{bt} = 0 \quad . \qquad (45)$$

Substitution of (45) into (37) would decouple the integral equations

(only unknown in (37a) is G_1 while the only unknown in (37b) is G_2) which would in turn enable us to solve them seperately. This property reduces both the computer time and memory space needed in the numerical solution.

2.5 Two Opposite Elliptic Edge Cracks

Two opposite edge cracks shown in Fig. 4 has exactly the same properties as symmetric internal cracks except for the coefficients of the shape functions. Once the shape functions are established by a suitable curve fitting, the same procedure that is applied to symmetric internal cracks is applied to find the stress intensity factors.

2.6 Interaction Between Two Identical Cracks

All the crack geometries that we considered up to now were single cracks lying in the region (-a,a) on the x_1 axis. Only difference among them was their configuration in the thickness

direction. Shape functions, energy available for fracture and functions α_{ij} and γ_{ij} are all sensitive to this configuration, while the form of the integral equation is independent of it. In this section, we will modify (1) and (2) for two identical cracks which is shown in Fig. 5. In this case D is defined as (b/a , c/a). With the new definition of D, (1) and (2) will take the following form.

$$\frac{\sigma(x')}{E} - \frac{1}{2\pi}\int_{b'}^{c'}\left[\frac{1}{z-x'} + \frac{1}{z+x'}\right]G_1(z)\,dz = \frac{\sigma_o}{E}, \quad b' < x' < c' , \tag{46}$$

$$\frac{m(x')}{E} - R_1\int_{b'}^{c'}\left[R_2\left[\frac{1}{z-x'} + \frac{1}{z+x'}\right] - R_3\left[\frac{1}{(z-x')^3} + \frac{1}{(z+x')^3}\right] + R_4\left[\frac{1}{z-x'}K_2(p|z-x'|) + \frac{1}{z+x'}K_2(p|z+x'|)\right]\right]G_2(z)\,dz$$

$$= \frac{m_o}{6E} \quad , \quad b' < x' < c' \quad , \tag{47}$$

where

$$x' = x_1/a, \qquad b' = b/a, \qquad c' = c/a .$$

Again we have to convert the limits of integrals to (-1,1) for

numerical solution purposes. By introducing the following parameters (keep in mind that from Fig. 5, (c'-b')/2 = 1)

$$x = (2x'-c'-b') / (c'-b') \quad , \tag{48}$$

$$x' = [(c'-b')x+c'+b'] / 2 = x + [(c'+b') / 2] \quad , \tag{49}$$

$$dx' = dx \quad ,$$

and

$$t = (2z-c'-b') / (c'-b') \quad , \tag{50}$$

$$z = [(c'-b')t+c'+b'] / 2 = t + [(c'+b') / 2] \quad , \tag{51}$$

$$dz = dt \quad ,$$

and substituting (27) and (28) for $\sigma(x)$ and m(x) respectively, (46) and (47) can be rewritten as follows:

$$\gamma_{bb}(x) \int_{-1}^{x} G_1(t)\, dt - R_1 \int_{-1}^{1} \left[R_2\left[\frac{1}{y_1} + \frac{1}{y_2}\right] - R_3\left[\frac{1}{y_1^3} + \frac{1}{y_2^3}\right] \right.$$

$$\left. + R_4\left[\frac{1}{y_1} K_2(p|y_1|) + \frac{1}{y_2} K_2(p|y_2|)\right] \right] G_1(t)\, dt + \gamma_{bt}(x) \int_{-1}^{x} G_2(t)\, dt$$

$$= \frac{m_o}{6E} \quad , \quad -1 < x < 1 \quad , \tag{52}$$

$$\tau_{tb}(x) \int_{-1}^{x} G_1(t)\, dt + \tau_{tt}(x) \int_{-1}^{x} G_2(t)\, dt - \frac{1}{2\pi} \int_{-1}^{1} \left[\frac{1}{y_1} + \frac{1}{y_2}\right] G_2(t)\, dt$$

$$= \frac{\sigma_o}{E} \quad , \quad -1 < x < 1 \quad , \tag{53}$$

where

$$y_1 = t - x \quad ,$$

$$y_2 = t + x + b' + c' \quad . \tag{54}$$

Integral equations (52) and (53) will again be solved by Gauss-Chebyshev closed form integration formula with the additional conditions

$$\int_{-1}^{1} G_1(t)\, dt = 0 \quad ,$$

$$\int_{-1}^{1} G_2(t)\, dt = 0 \quad ,$$

and the same backward procedure defined in Section 2.2 is used to find stress intensity factors at any point on the crack defined in

the region (b,c). Due to symmetry with respect to the x_2x_3 plane, stress intensity factors on the two cracks are also symmetric with respect to the same plane. Integral equations are valid for any two identical crack (edge, internal, two opposite) problem providing the corresponding γ functions defined in Section 2.2 .

2.7 Interaction of Three Identical Cracks

As stated earlier integral equations for general case given in (1) and (2) are valid for any number of cracks provided there is symmetry with respect to the x_2x_3 plane. This means that any three crack system composed of a symmetric crack surrounded by two identical cracks (not needed to be identical with the third one) can be solved by using (1) and (2). But in this study, for simplification purposes, all of them are chosen identical. Configuration and parameters are shown in Fig. 6. D is defined as (0,1), (b/a , c/a). Because of the nature of the problem, we expect that crack surface displacements and rotations be symmetric with respect to the x_2x_3 plane. This suggests that two outer cracks should have the same rotation and displacement at the equidistant points from the origin, while the third one undergoes completely different displacement and rotation. For this reason G functions

should be defined seperately for inner crack and two outer cracks.

Let

G_{11} : Crack surface rotation derivative for the inner crack, (-a,a),

G_{12} : Crack opening displacement derivative for the inner crack, (-a,a),

G_{21} : Crack surface rotation derivative for the outer crack, (b,c),

G_{22} : Crack opening displacement derivative for the outer crack, (b,c).

Also $\sigma(x)$ and $m(x)$ for the inner and outer cracks should be defined seperately as follows,

$\sigma_1(x)$: $\sigma(x)$ for inner crack,

$m_1(x)$: $m(x)$ for inner crack,

$\sigma_2(x)$: $\sigma(x)$ for outer crack,

$m_2(x)$: $m(x)$ for outer crack.

(1) and (2) can be written for inner crack

$$\frac{\sigma_1(x')}{E} - \frac{1}{2\pi}\int_0^1 \left[\frac{1}{z-x'} + \frac{1}{z+x'}\right] G_{11}(z)\, dz - \frac{1}{2\pi}\int_b^c \left[\frac{1}{z-x'}\right.$$

$$+\frac{1}{z+x'}\Big]\,G_{12}(z)\,dz=\frac{\sigma_o}{E}\quad,\quad 0<x'<1\,,\qquad(55)$$

$$\frac{m_1(x')}{6E}-R_1\int_0^1\Big[R_2\Big[\frac{1}{z-x'}+\frac{1}{z+x'}\Big]-R_3\Big[\frac{1}{(z-x')^3}+\frac{1}{(z+x')^3}\Big]$$

$$+R_4\Big[\frac{1}{z-x'}K_2(p\,z-x')+\frac{1}{z+x'}K_2(p\,z+x')\Big]\Big]G_{12}(z)\,dz$$

$$-R_1\int_{b'}^{c'}\Big[R_2\Big[\frac{1}{z-x'}+\frac{1}{z+x'}\Big]-R_3\Big[\frac{1}{(z-x')^3}+\frac{1}{(z+x')^3}\Big]$$

$$+R_4\Big[\frac{1}{z-x'}K_2(p|z-x'|)+\frac{1}{z+x'}K_2(p|z+x'|)\Big]\Big]G_{22}(z)\,dz$$

$$=\frac{m_o}{6E}\quad,\quad 0<x'<1\,,\qquad(56)$$

and for outer crack

$$\frac{\sigma_2(x')}{E}-\frac{1}{2\pi}\int_0^1\Big[\frac{1}{z-x'}+\frac{1}{z+x'}\Big]G_{11}(z)\,dz-\frac{1}{2\pi}\int_{b'}^{c'}\Big[\frac{1}{z-x'}$$

$$+\frac{1}{z+x'}\Big]\,G_{12}(z)\,dz=\frac{\sigma_o}{E},\quad b'<x'<c'\,,\qquad(57)$$

$$\frac{m_2(x')}{6E} - R_1 \int_0^1 \left[R_2 \left[\frac{1}{z-x'} + \frac{1}{z+x'} \right] - R_3 \left[\frac{1}{(z-x')^3} + \frac{1}{(z+x')^3} \right] \right.$$

$$\left. + R_4 \left[\frac{1}{z-x'} K_2(p|z-x'|) + \frac{1}{z+x'} K_2(p|z+x'|) \right] \right] G_{12}(z)\, dz$$

$$- R_1 \int_{b'}^{c'} \left[R_2 \left[\frac{1}{z-x'} + \frac{1}{z+x'} \right] - R_3 \left[\frac{1}{(z-x')^3} + \frac{1}{(z+x')^3} \right] \right.$$

$$\left. + R_4 \left[\frac{1}{z-x'} K_2(p|z-x'|) + \frac{1}{z+x'} K_2(p|z+x'|) \right] \right] G_{22}(z)\, dz$$

$$= \frac{m_o}{6E} \quad , \quad b' < x' < c' \, , \tag{58}$$

where $x' = x/a$, $b' = b/a$, $c' = c/a$.

From (36), we may write

$$\int_0^1 \left[\frac{1}{z-x'} + \frac{1}{z+x'} \right] G_{11}(z)\, dz = \int_{-1}^1 \frac{1}{z-x'} G_{11}(z)\, dz \quad , \tag{59}$$

$$\int_0^1 \left[R_2 \left[\frac{1}{z-x'} + \frac{1}{z+x'} \right. \right. - R_3 \left[\frac{1}{(z-x')^3} + \frac{1}{(z+x')^3} \right] + R_4 \left[\frac{1}{z-x'} K_2(p|z-x'|) \right.$$

$$+\frac{1}{z+x'}K_2(p|z+x'|)\Big]\Big]G_{12}(z)\,dz = \int_{-1}^{1}\Big[R_2\frac{1}{z-x'} - R_3\frac{1}{(z-x')^3}$$

$$+ R_4\frac{1}{z-x'}K_2(p|z-x'|)\Big]\,G_{12}(z)\,dz \quad . \qquad (60)$$

Same expressions as (59) and (60) can also be written for G_{21} and G_{22}.

If we define

$$x' = x \quad \text{for} \quad -1 < x' < 1 \quad ,$$
$$z = t \quad \text{for} \quad -1 < z < 1 \quad ,$$

and use (49) and (51) for $b' < x' < c'$ and $b' < z < c'$ respectively, and substitute (27), (28) for $\sigma(x)$ and $m(x)$, (55), (56), (57), (58) will take the following final form.

$$\gamma_{bb}(x)\int_{-1}^{x}G_{21}(t)\,dt - R_1\int_{-1}^{1}\Big[R_2\Big[\frac{1}{y_1}+\frac{1}{y_2}\Big] - R_3\Big[\frac{1}{y_1^3}+\frac{1}{y_2^3}\Big]$$

$$+ R_4\Big[\frac{1}{y_1}K_2(p|y_1|) + \frac{1}{y_2}K_2(p|y_2|)\Big]\Big]\,G_{21}(t)\,dt - R_1\int_{-1}^{1}\Big[R_2\frac{1}{y_3}$$

$$- R_3 \frac{1}{y_3^3} + R_4 \frac{1}{y_3} K_2(p|y_3|) \Big] G_{11}(t)\, dt + \gamma_{bt}(x) \int_{-1}^{x} G_{22}(t)\, dt$$

$$= \frac{m_o}{6E} \quad , \quad -1 < x < 1 \, , \tag{61}$$

$$\gamma_{tb}(x) \int_{-1}^{x} G_{21}(t)\, dt + \gamma_{tt}(x) \int_{-1}^{x} G_{22}(t)\, dt - \frac{1}{2\pi} \int_{-1}^{1} \Big[\frac{1}{y_1}$$

$$+ \frac{1}{y_2} \Big] G_{22}(t)\, dt - \frac{1}{2\pi} \int_{-1}^{1} \frac{1}{y_3} G_{12}(t)\, dt = \frac{\sigma_o}{E} \, , \quad -1 < x < 1, \tag{62}$$

$$\gamma_{bb}(x) \int_{-1}^{x} G_{11}(t)\, dt - R_1 \int_{-1}^{1} \Big[R_2 \Big[\frac{1}{y_4} + \frac{1}{y_5} \Big] - R_3 \Big[\frac{1}{y_4^3} + \frac{1}{y_5^3} \Big]$$

$$+ R_4 \Big[\frac{1}{y_4} K_2(p\, y_4) + \frac{1}{y_5} K_2(p\, y_5) \Big] \Big] G_{21}(t)\, dt - R_1 \int_{-1}^{1} \Big[R_2 \frac{1}{y_1}$$

$$- R_3 \frac{1}{y_1^3} + R_4 \frac{1}{y_1} K_2(p\, y_1) \Big] G_{11}(t)\, dt + \gamma_{bt}(x) \int_{-1}^{x} G_{12}(t)\, dt$$

$$= \frac{m_o}{6E} \quad , \quad -1 < x < 1 \, , \tag{63}$$

$$\gamma_{tb}(x) \int_{-1}^{x} G_{11}(t)\, dt + \gamma_{tt}(x) \int_{-1}^{x} G_{12}(t)\, dt - \frac{1}{2\pi} \int_{-1}^{1} \Big[\frac{1}{y_4}$$

$$+\frac{1}{y_5}\Big]\, G_{22}(t)\, dt - \frac{1}{2\pi}\int_{-1}^{1}\frac{1}{y_1}\, G_{12}(t)\, dt = \frac{\sigma_o}{E}\ , \quad -1 < x < 1\ , \quad (64)$$

where
$$y_1 = t-x \quad ,$$
$$y_2 = t+x+b'+c' \quad ,$$
$$y_3 = t-x-[(b'+c')/2] \quad ,$$
$$y_4 = t+x+[(b'+c')/2] \quad ,$$
$$y_5 = t-x+[(b'+c')/2] \quad .$$

This problem has four integral equations, (61), (62), (63), (64), with four unknown functions, G_{11}, G_{12}, G_{21}, G_{22}, which will be solved by Gauss-Chebyshev closed type integration formula under the following single-valuedness conditions.

$$\int_{-1}^{1} G_{11}(t)\, dt = 0 \quad ,$$
$$\int_{-1}^{1} G_{12}(t)\, dt = 0 \quad ,$$
$$\int_{-1}^{1} G_{21}(t)\, dt = 0 \quad ,$$
$$\int_{-1}^{1} G_{22}(t)\, dt = 0 \quad .$$

After solving for the unknown functions, the same backward procedure

defined in Section 2.2 will be used for each crack seperately in order to find stress intensity factors.

Provided the corresponding γ functions, equations (61), (62), (63), (64) can be applied to any type(edge, internal, collinear) of identical cracks. The only reason for considering identical cracks to demonstrate interaction of three cracks in this section is simplicity. Line-spring model can also be applied to any three crack system which has two outer identical cracks with another symmetric(with respect to the x_2x_3 plane) crack in the middle. In this case, γ functions and crack length will be defined seperately for both(outer ones and inner one) cracks. One should keep in mind that crack length is a parameter in the coefficients of (61), (62), (63), (64). Attention must be paid to redifine the coefficients in such case.

3. RESULTS AND DISCUSSION

There are two main objectives in this study:

1. Assess the accuracy of line spring model,
2. Provide extensive numerical results which may be useful in application.

Due to unavailability of the solutions for the cases that we are interested in, the first objective can only be reached for the central (d/h=0) elliptic internal crack under pure tension. Extensive results for central, eccentric internal cracks and two opposite edge cracks as well as the interaction among two and three cracks are tabulated. In all cases it was assumed that ν=0.3 . However, the effect of ν on the stress intensity factors does not seem to be significant.

First step for the application of line spring model is to represent the SIFs as a polynomial in L/h. For this purpose, extensive information about plane strain (a/L_o) stress intensity factors are needed. These results are obtained from previous materials for internal cracks, from [18] for two opposite edge cracks and are tabulated in Tables 1,3,5,7,9,11,13,15. Corresponding coefficients of shape functions are tabulated in Tables 2,4,6,8,10,12,14,16. Coefficients of shape functions for the edge crack case are directly taken from [1] and tabulated in Table 17.

As noted before, for the application of the line spring model, the contour of the part-through crack can be any reasonable curve. Elliptic cracks are studied here since it is believed that ellipse is the closest contour for the actual shape of the crack which may be encountered in practical applications. Thus, crack length for any cross section is defined by,

$$L(x_1) = L_o\sqrt{1 - (x_1/a)^2} = L_o\sqrt{1 - x^2}$$

L_o being the total crack length at the midsection (x=0) . Note that the limiting values of the SIF are

$$K \to 0 \quad \text{for} \quad a/h \to 0 \quad ; \quad K \to K_\infty \quad \text{for} \quad a/h \to \infty$$

The first case that is studied is the central internal elliptic crack (d/h=0). Extensive results and formulas developed from a finite element method for this case are given in [19]. Table 18 and Figs. 19,20 show the comparision of the SIFs obtained from this study with those generated from the formulas given in [19]. SIFs obtained from [19] are represented as K^r while the normalizing SIF is $K_o = \sigma_o\sqrt{\pi L_o/2}$ where $\sigma_o = N_{22}^{\infty}/h$. Both values and the percent differences between them are given for various parameters at x=0 and x=1/2 . As expected, the SIFs $K(L_o)$ for the elliptic crack are

consistently smaller than the plane strain values. The table shows that with the exception of relatively small values of a/L_o at small L_o/h (for which the line spring is really not a suitable model) the agreement is surprisingly good. From the results, one may conclude that line spring can be used with some confidence for any central internal elliptic crack which has an a/L_o ratio larger than 2.

SIFs for the same geometry, but under pure bending are given in Table 20 (Fig. 21). This time, normalizing SIF is defined as $K_o = m_o(\pi L_o/2)^{1/2}$ where $m_o = 6M_{22}^{\infty}/h$. The results given are for the tension side. On the compression side the stress intensity factors have the same values with a negative sign. Under pure bending, since the crack faces on the compression side of the plate would close, the results given in the table cannot be used seperately. The results are, of course, useful and valid if the plate is subjected to tension, as well as bending, in such a way that the superimposed SIF is positive everywhere.

From Table 20, by excluding the case of $a/L_o=0.5$ which proved to be unreliable, it may be concluded that SIF are independent of a/L_o ratio for $L_o/h < 0.5$. For $L_o/h > 0.5$, SIF begins to increase with increasing L_o/h ratio, which is expected. Though we are unable to confirm the accuracy of the line spring model in this case, we could say that there is no unusual behaviour in the results. Results are asymptotically approaching to plane strain values as a/L_o is

increased except for large L_o/h values.

Another comparision with the previous finite element results [20] is shown in Table 19 (Fig. 23). It should be noted that in the results given in Table 19 $a/L_o=1.25$ is relatively small for the line spring model to be effective. Despite that, the relative error does not seem to be very high.

After symmetric internal cracks, nonsymmetrically located internal cracks are studied both under pure tension and pure bending conditions. Extensive results which scan almost all possible configurations are given in Tables 21-32 (Figs. 7-18). Normalizing SIFs are the same as that defined in the previous case for both tension and bending. Again we are unable to verify in which region the line spring results are reliable because of the lack of previous work done on this kind of problem. Asymptotic convergence to plane strain results is fairly good. A close observation of the tension results would show that for small a/L_o ratios SIFs first decrease, then increase with increasing L_o/h. This is mainly due to the fact that tabulated results are normalized with respect to $\sigma_o\sqrt{\pi L_o/2}$. Thus, even though the normalized SIF is decreasing, the real SIF may increase (which indeed happens in this case) but with a lower rate than the rate of increase of L_o . Also, again for small L_o/h and a/L_o values SIF on the inside part of the crack front turns out to be greater than that on the other part of the crack border which is

closer to the free surface.

Two opposite elliptic edge cracks have been studied only under pure tension. Normalizing stress intensity factor is again $\sigma_o (\pi L_o/2)^{1/2}$ with $\sigma_o = N_{22}^{\infty}/h$. Decreasing-increasing behaviour of the SIFs is again observed here. Same explanation which is given earlier is also valid for this case. Plane strain results are very close to each other in the region that we observe the slight decrease in SIFs. For this reason, a small uncertainity in the calculations can easily result with a slight decrease while we are expecting a slight increase. Except this behaviour, everything is as expected in Table 33 (Fig. 22).

Results for the interaction of two identical elliptic internal cracks under pure bending and pure tension have been tabulated in Tables 34 and 35 respectively. It can be seen that there is almost no interaction between two identical elliptic edge cracks if the distance between them (Fig.5) is larger than 8 times the half crack length, a. Another result which may be observed is that the interaction is more effective for the cracks having large L_o/h ratios.

SIFs for the two identical central internal elliptic cracks are tabulated in Table 36. Results are given only for tension case because it has been observed that there is no appreciable

interaction for the crack geometries given in Table 36 under pure bending. SIF deviates not more than 1% from the single crack value for b/a=0.1 in bending. It is seen that as the distance between the two cracks is increased the single crack solution is easily recovered. There is almost no interaction for $b/a \geq 0.1$ for the cracks $L_o/h < 0.5$. If $L_o/h > 0.5$, no interaction region can be defined for $b/a \geq 4$.

Interaction results for any two identical elliptic internal cracks are given in Table 37. Some erratic results are observed for small a/L_o ratios at small L_o/h ratios. Clearly, for these crack geometries line spring is not a suitable model.

As the last example, SIFs for the three identical internal elliptic cracks under pure tension are calculated and are given in Table 38. The only conclusion one may draw from these results is that the SIFs on the middle crack are slightly higher than the SIFs on the outer crack. But the difference is so small that they may be regarded as equal.

T A B L E S

Table 1. Stress intensity factors for centrally cracked plate subjected to tension N or bending M under plane strain conditions.

L/h	$(K/K_o)_N$	$(K/K_o)_M$
0.05		0.0250
0.1	1.0060	0.0500
0.2	1.0246	0.1001
0.3	1.0577	0.1505
0.4	1.1094	0.2023
0.5	1.1867	0.2573
0.6	1.3033	0.3197
0.7	1.4884	0.3986
0.8	1.8169	0.5186
0.9	2.585	0.7776
0.95	4.252	1.1421

Table 2. The coefficients b_i and c_i for the shape functions g_t and g_b for symmetric internal (d/h=0) crack.

i	b_i	c_i
1	0.7070	0.0169
2	0.4325	-0.4629
3	-0.1091	15.0622
4	7.3711	-143.7384
5	-57.7894	807.2449
6	271.1551	-2844.8525
7	-744.4204	6468.9152
8	1183.9529	-9477.5512
9	-1001.4920	8638.7826
10	347.9786	-4455.2167
11		993.2482

Table 3. Stress intensity factors for the plate which has an internal crack with d/h=0.05 subjected to uniform tension N or bending M under plane strain conditions.

L/h	$(K_A/K_o)_N$	$(K_B/K_o)_N$	$(K_A/K_o)_M$	$(K_B/K_o)_M$
0.0001			0.1001	0.1000
0.09	1.0053	1.0050	0.1455	0.0555
0.18	1.0221	1.0200	0.1923	0.0120
0.27	1.0530	1.0452	0.2409	-0.0305
0.36	1.1021	1.0823	0.2925	-0.0722
0.45	1.1769	1.1340	0.3497	-0.1134
0.54	1.2909	1.2053	0.4175	-0.1547
0.63	1.4731	1.3053	0.5068	-0.1973
0.72	1.7983	1.4518	0.6467	-0.2430
0.81	2.5631	1.6887	0.9525	-0.2923
0.855	3.6610	1.8858	1.3814	-0.3125

Table 4. The coefficients of b_i and c_i for the shape functions g_t and g_b for internal crack with d/h=0.05.

i	b_{Ai}	b_{Bi}	c_{Ai}	c_{Bi}
1	0.7071	0.7071	0.0708	0.0707
2	0.4597	0.4347	-0.0623	-0.3701
3	0.7671	-0.0915	13.1229	0.5654
4	0.1552	2.6973	-166.4280	-6.6423
5	-9.3017	-14.1195	1145.8217	45.7189
6	97.3172	54.9653	-4762.0914	-189.9515
7	-413.9673	-135.3432	12511.5152	498.8463
8	936.4719	205.3051	-20927.0019	-834.5704
9	-1078.2322	-173.3480	21613.9362	862.1672
10	504.0555	62.8847	-12568.0268	-501.4354
11			3148.4879	125.5869

Table 5. Stress intensity factors for the plate which has an internal crack with d/h=0.10 subjected to uniform tension N or bending M under plane strain conditions.

L/h	$(K_A/K_o)_N$	$(K_B/K_o)_N$	$(K_A/K_o)_M$	$(K_B/K_o)_M$
0.0001			0.2001	0.2000
0.08	1.0050	1.0046	0.2410	0.1609
0.16	1.0212	1.0179	0.2843	0.1236
0.24	1.0513	1.0399	0.3308	0.0881
0.32	1.0998	1.0709	0.3821	0.0545
0.40	1.1743	1.1126	0.4410	0.0231
0.48	1.2887	1.1677	0.5136	-0.0059
0.56	1.4722	1.2418	0.6123	-0.0313
0.64	1.8002	1.3465	0.7701	-0.0504
0.72	2.5705	1.5167	1.1183	-0.0519
0.76	3.6693	1.6727	1.6050	-0.0280

Table 6. The coefficients of b_i and c_i for the shape functions g_t and g_b for internal crack with d/h=0.10.

i	b_{Ai}	b_{Bi}	c_{Ai}	c_{Bi}
1	0.7071	0.7072	0.1415	0.1414
2	0.5498	0.5043	-0.1734	-0.3871
3	1.5235	-0.5779	18.7434	1.2936
4	-2.2395	7.6480	-266.7713	-17.0715
5	-5.2844	-52.8793	2066.4692	132.0282
6	226.0267	257.2074	-9661.5218	-617.3023
7	-1423.2887	-799.7410	28556.2764	1826.3191
8	4348.1446	1530.8314	-53734.1216	-3441.9797
9	-6553.5540	-1634.0240	62435.9340	4007.6642
10	3959.2116	749.0673	-40844.2364	-2628.6642
11			11511.5912	743.3343

Table 7. Stress intensity factors for the plate which has an internal crack with d/h=0.15 subjected to uniform tension N or bending M under plane strain conditions.

L/h	$(K_A/K_o)_N$	$(K_B/K_o)_M$	$(K_A/K_o)_M$	$(K_B/K_o)_M$
0.0001			0.3001	0.3000
0.07	1.0049	1.0045	0.3365	0.2663
0.14	1.0208	1.0172	0.3763	0.2352
0.21	1.0506	1.0380	0.4206	0.2066
0.28	1.0988	1.0671	0.4714	0.1807
0.35	1.1729	1.1057	0.5319	0.1580
0.42	1.2868	1.1561	0.6089	0.1395
0.49	1.4693	1.2235	0.7164	0.1271
0.56	1.7938	1.3197	0.8909	0.1259
0.63	2.5476	1.4829	1.2760	0.1533
0.665	3.6065	1.6426	1.8090	0.2032

Table 8. The coefficients of b_i and c_i for the shape functions g_t and g_b for internal crack with d/h=0.15.

i	b_{Ai}	b_{Bi}	c_{Ai}	c_{Bi}
1	0.7071	0.7072	0.2122	0.2121
2	0.7028	0.6376	-0.2929	-0.4042
3	2.7653	-1.2331	26.3239	2.2494
4	-7.2036	19.0057	-427.2558	-33.6757
5	9.1384	-173.8407	3782.9591	297.4990
6	667.4954	1108.9410	-20214.1250	-1590.1109
7	-6105.7233	-4517.1019	68285.5344	5378.6049
8	25260.2847	11317.3469	-146859.5866	-11588.2217
9	-50586.0954	-15802.5485	195038.2341	15425.1699
10	40325.8388	9475.7480	-145833.6228	-11566.8288
11			46980.5243	3740.3538

Table 9. Stress intensity factors for the plate which has an internal crack with d/h=0.20 subjected to uniform tension N or bending M under plane strain conditions.

L/h	$(K_A/K_o)_N$	$(K_B/K_o)_N$	$(K_A/K_o)_M$	$(K_B/K_o)_M$
0.0001			0.4001	0.4000
0.06	1.0048	1.0044	0.4319	0.3718
0.12	1.0205	1.0170	0.4682	0.3468
0.18	1.0497	1.0374	0.5102	0.3252
0.24	1.0968	1.0660	0.5601	0.3070
0.30	1.1691	1.1034	0.6216	0.2930
0.36	1.2799	1.1535	0.7020	0.2844
0.42	1.4562	1.2202	0.8162	0.2839
0.48	1.7668	1.3161	1.0031	0.2981
0.54	2.4756	1.4806	1.4127	0.3482
0.57	3.4498	1.6422	1.9674	0.4165

Table 10. The coefficients of b_i and c_i for the shape functions g_t and g_b for internal crack with d/h=0.20.

i	b_{Ai}	b_{Bi}	c_{Ai}	c_{Bi}
1	0.7071	0.7072	0.2829	0.2828
2	0.9394	0.8534	-0.4105	-0.4192
3	5.0186	-2.2518	36.3675	3.4524
4	-19.6345	47.2610	-686.9924	-59.3848
5	76.1489	-589.3736	7097.1745	611.7194
6	2376.8770	5125.5432	-44245.1037	-3814.7743
7	-32402.0663	-28413.7181	174386.6733	15058.0019
8	187563.3073	96818.0664	-437594.1661	-37860.2290
9	-517758.7465	-183743.9141	678087.6506	58816.9514
10	566112.6482	149736.5141	-591607.7634	-51479.6217
11			222394.8277	19433.7456

Table 11. Stress intensity factors for the plate which has an internal crack with d/h=0.25 subjected to uniform tension N or bending M under plane strain conditions.

L/h	$(K_A/K_o)_N$	$(K_B/K_o)_N$	$(K_A/K_o)_M$	$(K_B/K_o)_M$
0.0001			0.5001	0.5000
0.05	1.0046	1.0042	0.5273	0.4771
0.10	1.0197	1.0165	0.5598	0.4583
0.15	1.0476	1.0364	0.5991	0.4434
0.20	1.0925	1.0644	0.6473	0.4327
0.25	1.1610	1.1016	0.7084	0.4270
0.30	1.2652	1.1505	0.7900	0.4277
0.35	1.4295	1.2160	0.9074	0.4380
0.40	1.7151	1.3099	1.0996	0.4649
0.45	2.3529	1.4684	1.5149	0.5310
0.475	3.2077	1.6192	2.0658	0.6085

Table 12. The coefficients of b_i and c_i for the shape functions g_t and g_b for internal crack with d/h=0.25.

i	b_{Ai}	b_{Bi}	c_{Ai}	c_{Bi}
1	0.7071	0.7071	0.3536	0.3536
2	1.3041	1.1918	-0.5246	-0.4284
3	9.6510	-4.1793	50.2589	4.8592
4	-57.8163	129.7358	-1136.1027	-97.6558
5	450.7761	-2325.3551	14085.0245	1206.5210
6	10351.8621	29069.6053	-105370.0173	-9029.9162
7	-227973.9193	-231101.0011	498386.1475	42788.3389
8	1960136.6080	1128028.3541	-1500844.1305	-129153.3052
9	-7899243.5583	-3063223.0225	2791092.0497	240895.9775
10	12538854.7550	3568834.5097	-2922538.2779	-253169.5873
11			1318591.9416	114779.2965

Table 13. Stress intensity factors for the plate which has an internal crack with d/h=0.30 subjected to uniform tension N or bending M under plane strain conditions.

L/h	$(K_A/K_o)_N$	$(K_B/K_o)_N$	$(K_A/K_o)_M$	$(K_B/K_o)_M$
0.001			0.6001	0.6000
0.04	1.0043	1.0040	0.6226	0.5824
0.08	1.0183	1.0155	0.6510	0.5686
0.12	1.0442	1.0343	0.6867	0.5607
0.16	1.0855	1.0608	0.7320	0.5568
0.20	1.1481	1.0959	0.7909	0.5584
0.24	1.2425	1.1419	0.8708	0.5669
0.28	1.3898	1.2031	0.9866	0.5855
0.32	1.6423	1.2895	1.1755	0.6209
0.36	2.1937	1.4309	1.5773	0.6939
0.38	2.9157	1.5591	2.0992	0.7709

Table 14. The coefficients of b_i and c_i for the shape functions g_t and g_b for internal crack with d/h=0.30.

i	b_{Ai}	b_{Bi}	c_{Ai}	c_{Bi}
1	0.7071	0.7071	0.4244	0.4243
2	1.9027	1.7480	-0.6553	-0.4321
3	20.8636	-8.9087	72.3179	6.6403
4	-197.8895	440.7103	-2037.1553	-160.0429
5	2675.1513	-12390.9668	31569.7505	2468.7747
6	71601.3880	241718.2677	-295202.5115	-23090.8486
7	-2639273.5314	-2989605.6659	1745346.7908	136788.4159
8	35994016.1511	22618755.1306	-6570139.7052	-516213.4074
9	-227958779.2155	-94950523.9757	15273818.2302	1203928.2026
10	567162515.8604	170542044.2578	-19993047.6604	-1582260.0614
11			11276922.9053	897240.7983

Table 15. Stress intensity factors for the plate with collinear edge cracks subjected to uniform tension N under plane strain conditions.

L/h	$(K/K_o)_N$
0.0001	1.1221
0.1	1.1231
0.2	1.1254
0.3	1.1292
0.4	1.1370
0.5	1.1546
0.6	1.2117
0.7	1.3254
0.8	1.5393
0.9	2.0836

Table 16. The coefficients of b_i for the shape function g_t for collinear edge crack.

i	b_i
1	0.7934
2	0.0775
3	-0.7542
4	7.5825
5	-12.1712
6	-186.5011
7	1236.2858
8	-3043.6190
9	3350.3456
10	-1374.8426

Table 17. The coefficients of b_i and c_i for the shape functions g_t and g_b for edge crack.

i	b_i	c_i
1	1.1216	1.1202
2	6.5200	-1.8872
3	-12.3877	18.0143
4	89.0554	-87.3851
5	-188.6080	241.9124
6	207.3870	-319.9402
7	-32.0524	168.0105

Table 18. Comparison of the stress intensity factors K(x) calculated in this study at x=0 and x=1/2 ($x=x_1/a$) for an internal planar elliptic crack in a plate under uniform tension N with the corresponding values $K^r(x)$ given in Ref.[19] . $\%D=100(K^r-K)/K^r$.

L_o/h	a/L_o	x	$K(x)/K_o$	$K^r(x)/K_o$	%D
0.1	0.5	0	0.916	0.637	43.7
0.1	0.5	1/2	0.868	0.637	36.2
0.1	1.0	0	0.955	0.827	15.5
0.1	1.0	1/2	0.896	0.785	14.2
0.1	2.0	0	0.976	0.935	4.3
0.1	2.0	1/2	0.911	0.875	4.1
0.1	3.0	0	0.983	0.967	1.7
0.1	3.0	1/2	0.916	0.902	1.6
0.1	4.0	0	0.987	0.980	0.6
0.1	4.0	1/2	0.919	0.914	0.5
0.1	10.0	0	0.993	0.999	-0.6
0.1	10.0	1/2	0.923	0.930	-0.7
0.2	0.5	0	0.862	0.638	35.1
0.2	0.5	1/2	0.827	0.638	29.6
0.2	1.0	0	0.931	0.830	12.2
0.2	1.0	1/2	0.880	0.788	11.6
0.2	2.0	0	0.971	0.942	3.1
0.2	2.0	1/2	0.908	0.881	3.1
0.2	3.0	0	0.986	0.976	1.0
0.2	3.0	1/2	0.918	0.910	0.9
0.2	4.0	0	0.993	0.991	0.2
0.2	4.0	1/2	0.923	0.923	0.0
0.2	10.0	0	1.007	1.013	-0.6
0.2	10.0	1/2	0.933	0.942	-1.0

Table 18- Cont.

L_o/h	a/L_o	x	$K(x)/K_o$	$K^r(x)/K_o$	%D
0.3	0.5	0	0.824	0.641	28.6
0.3	0.5	1/2	0.796	0.640	24.4
0.3	1.0	0	0.920	0.837	9.9
0.3	1.0	1/2	0.871	0.794	9.8
0.3	2.0	0	0.979	0.957	2.3
0.3	2.0	1/2	0.914	0.893	2.3
0.3	3.0	0	1.001	0.996	0.5
0.3	3.0	1/2	0.930	0.927	0.3
0.3	4.0	0	1.012	1.014.	-0.2
0.3	4.0	1/2	0.937	0.942	-0.5
0.3	10.0	0	1.034	1.041	-0.7
0.3	10.0	1/2	0.952	0.966	-1.5
0.4	0.5	0	0.798	0.645	23.6
0.4	0.5	1/2	0.775	0.644	20.3
0.4	1.0	0	0.920	0.851	8.1
0.4	1.0	1/2	0.871	0.804	8.3
0.4	2.0	0	1.000	0.984	1.6
0.4	2.0	1/2	0.929	0.915	1.6
0.4	3.0	0	1.030	1.031	-0.1
0.4	3.0	1/2	0.950	0.955	-0.4
0.4	4.0	0	1.047	1.054	-0.7
0.4	4.0	1/2	0.961	0.974	-1.3
0.4	10.0	0	1.078	1.091	-1.2
0.4	10.0	1/2	0.982	1.005	-2.3

Table 18- Cont.

L_o/h	a/L_o	x	$K(x)/K_o$	$K^r(x)/K_o$	%D
0.5	0.5	0	0.783	0.654	19.8
0.5	0.5	1/2	0.761	0.650	17.2
0.5	1.0	0	0.932	0.874	6.7
0.5	1.0	1/2	0.880	0.821	7.3
0.5	2.0	0	1.036	1.030	0.6
0.5	2.0	1/2	0.956	0.949	0.7
0.5	3.0	0	1.078	1.090	-1.1
0.5	3.0	1/2	0.984	0.998	-1.4
0.5	4.0	0	1.101	1.121	-1.8
0.5	4.0	1/2	0.998	1.023	-2.4
0.5	10.0	0	1.145	1.172	-2.4
0.5	10.0	1/2	1.025	1.063	-3.5
0.6	0.5	0	0.779	0.667	16.9
0.6	0.5	1/2	0.756	0.658	14.9
0.6	1.0	0	0.960	0.911	5.4
0.6	1.0	1/2	0.901	0.846	6.4
0.6	2.0	0	1.095	1.103	-0.8
0.6	2.0	1/2	0.997	0.999	-0.2
0.6	3.0	0	1.151	1.183	-2.7
0.6	3.0	1/2	1.033	1.061	-2.6
0.6	4.0	0	1.183	1.225	-3.5
0.6	4.0	1/2	1.052	1.092	-3.6
0.6	10.0	0	1.245	1.298	-4.0
0.6	10.0	1/2	1.088	1.143	-4.7

Table 18- Cont.

L_o/h	a/L_o	x	$K(x)/K_o$	$K^r(x)/K_o$	%D
0.7	0.5	0	0.788	0.687	14.7
0.7	0.5	1/2	0.760	0.671	13.3
0.7	1.0	0	1.009	0.968	4.3
0.7	1.0	1/2	0.935	0.882	6.0
0.7	2.0	0	1.187	1.213	-2.2
0.7	2.0	1/2	1.058	1.067	-0.8
0.7	3.0	0	1.266	1.322	-4.2
0.7	3.0	1/2	1.106	1.144	-3.3
0.7	4.0	0	1.310	1.381	-5.1
0.7	4.0	1/2	1.132	1.183	-4.4
0.7	10.0	0	1.403	1.483	-5.4
0.7	10.0	1/2	1.179	1.242	-5.1
0.8	0.5	0	0.818	0.717	14.1
0.8	0.5	1/2	0.777	0.686	12.9
0.8	1.0	0	1.096	1.051	4.3
0.8	1.0	1/2	0.991	0.930	6.6
0.8	2.0	0	1.341	1.372	-2.3
0.8	2.0	1/2	1.152	1.152	0.0
0.8	3.0	0	1.457	1.521	-4.3
0.8	3.0	1/2	1.218	1.245	-2.2
0.8	4.0	0	1.525	1.603	-4.9
0.8	4.0	1/2	1.253	1.290	-2.9
0.8	10.0	0	1.674	1.747	-4.2
0.8	10.0	1/2	1.318	1.349	-2.3

Table 18- Cont.

L_o/h	a/L_o	x	$K(x)/K_o$	$K^r(x)/K_o$	%D
0.9	0.5	0	0.905	0.759	19.3
0.9	0.5	1/2	0.813	0.709	14.7
0.9	1.0	0	1.284	1.167	10.0
0.9	1.0	1/2	1.086	0.987	10.1
0.9	2.0	0	1.661	1.594	4.2
0.9	2.0	1/2	1.310	1.246	5.1
0.9	3.0	0	1.858	1.799	3.3
0.9	3.0	1/2	1.405	1.347	4.2
0.9	4.0	0	1.981	1.912	3.6
0.9	4.0	1/2	1.456	1.392	4.6

Table 19. Comparison of the stress intensity factors $K(L_o)$ calculated in this study at the midsection of a symmetrically located internal(d/h=0) planar crack in a plate under uniform tension N with the corresponding results K^r given in [20]. $L_o/h=.75$, $a/L_o=1.25$, $x=x_1/a=\cos\theta$, $\%D=100(K-K^r)/K^r$.

θ	x	K^r/K_o	K/K_o	%D
90°	0	0.985	1.120	13.7
80°	0.174	0.971	1.103	13.6
70°	0.342	0.944	1.052	11.4
60°	0.500	0.898	0.973	8.4
45°	0.707	0.810	0.832	2.7
40°	0.766	0.770	0.742	-3.6

Table 20. Normalized stress intensity factors calculated at the midsection of a symmetrically located (d/h=0) internal planar elliptic crack in a plate under uniform bending M.

L_0/h \ $a/L_0 \rightarrow$	0.5	2.0	3.0	4.0	5.0	10.0	Plane Strain
0.1	.050	.050	.050	.050	.050	.050	.050
0.2	.099	.099	.099	.099	.099	.099	.100
0.3	.148	.149	.149	.149	.149	.149	.151
0.4	.195	.199	.199	.199	.200	.200	.202
0.5	.240	.250	.251	.252	.253	.254	.257
0.6	.285	.305	.308	.310	.311	.313	.320
0.7	.332	.369	.375	.379	.382	.387	.399
0.8	.387	.457	.470	.478	.483	.496	.519
0.9	.476	.619	.650	.670	.683	.717	.778

Table 21. Normalized stress intensity factors calculated at the midsection of an internal planar elliptic crack with d/h=.05 in a plate under uniform tension N.

K_A/K_o

L_o/h \ a/L_o →	0.5	1.0	2.0	3.0	4.0	7.0	10.0	Plane Strain
.05	0.954	0.975	0.987	0.990	0.992	0.995	0.996	1.002
.15	0.887	0.944	0.976	0.988	0.994	1.001	1.004	1.015
.25	0.838	0.926	0.979	0.998	1.008	1.022	1.028	1.045
.35	0.804	0.921	0.996	1.025	1.040	1.061	1.070	1.096
.45	0.782	0.931	1.032	1.073	1.095	1.126	1.139	1.177
.55	0.775	0.959	1.096	1.153	1.185	1.231	1.251	1.307
.65	0.786	1.018	1.204	1.288	1.336	1.407	1.439	1.529
.75	0.828	1.134	1.407	1.539	1.619	1.742	1.799	1.970
.85	0.994	1.479	1.987	2.268	2.452	2.761	2.921	3.481

K_B/K_o

L_o/h \ a/L_o →	0.5	1.0	2.0	3.0	4.0	7.0	10.0	Plane Strain
.05	0.955	0.976	0.987	0.991	0.993	0.995	0.996	1.002
.15	0.891	0.946	0.977	0.988	0.993	1.001	1.003	1.014
.25	0.847	0.929	0.978	0.996	1.006	1.018	1.023	1.039
.35	0.817	0.923	0.991	1.017	1.031	1.049	1.056	1.078
.45	0.798	0.928	1.017	1.051	1.070	1.095	1.105	1.134
.55	0.789	0.944	1.056	1.102	1.127	1.161	1.176	1.215
.65	0.788	0.972	1.115	1.176	1.210	1.257	1.277	1.333
.75	0.797	1.017	1.201	1.284	1.332	1.401	1.432	1.517
.85	0.822	1.088	1.334	1.455	1.529	1.643	1.697	1.859

Table 22. Normalized stress intensity factors calculated at the midsection of an internal planar elliptic crack with d/h=0.10 in a plate under uniform tension N.

K_A/K_o

L_o/h \ a/L_o→	0.5	1.0	2.0	3.0	4.0	7.0	10.0	Plane Strain
.05	0.950	0.974	0.986	0.990	0.992	0.995	0.996	1.002
.15	0.878	0.940	0.975	0.988	0.994	1.003	1.006	1.018
.25	0.825	0.921	0.980	1.002	1.013	1.029	1.036	1.056
.35	0.789	0.919	1.004	1.037	1.055	1.081	1.092	1.124
.45	0.770	0.937	1.056	1.105	1.132	1.172	1.189	1.240
.55	0.770	0.986	1.152	1.226	1.268	1.331	1.360	1.444
.65	0.805	1.093	1.342	1.462	1.534	1.646	1.699	1.860
.75	0.961	1.426	1.900	2.159	2.329	2.615	2.764	3.291

K_B/K_o

L_o/h \ a/L_o→	0.5	1.0	2.0	3.0	4.0	7.0	10.0	Plane Strain
.05	0.952	0.974	0.986	0.990	0.993	0.995	0.996	1.002
.15	0.886	0.943	0.976	0.988	0.993	1.001	1.005	1.016
.25	0.843	0.927	0.979	0.998	1.007	1.021	1.026	1.043
.35	0.815	0.923	0.993	1.020	1.034	1.054	1.062	1.085
.45	0.798	0.928	1.019	1.055	1.075	1.102	1.113	1.145
.55	0.789	0.944	1.059	1.107	1.133	1.171	1.187	1.231
.65	0.788	0.970	1.116	1.181	1.218	1.272	1.296	1.363
.75	0.795	1.010	1.203	1.297	1.355	1.445	1.488	1.625

Table 23. Normalized stress intensity factors calculated at the midsection of an internal planar elliptic crack with d/h=0.15 in a plate under uniform tension N.

K_A/K_o

L_o/h \ a/L_o→	0.5	1.0	2.0	3.0	4.0	7.0	10.0	Plane Strain
.05	0.944	0.971	0.985	0.989	0.992	0.995	0.996	1.002
.15	0.864	0.934	0.974	0.988	0.996	1.006	1.010	1.024
.25	0.808	0.916	0.984	1.009	1.022	1.041	1.049	1.076
.35	0.773	0.921	1.020	1.060	1.083	1.115	1.129	1.173
.45	0.761	0.956	1.101	1.164	1.200	1.254	1.279	1.354
.55	0.784	1.051	1.273	1.378	1.441	1.540	1.588	1.733
.65	0.926	1.362	1.789	2.021	2.172	2.427	2.560	3.033

K_B/K_o

L_o/h \ a/L_o→	0.5	1.0	2.0	3.0	4.0	7.0	10.0	Plane Strain
.05	0.964	0.972	0.985	0.990	0.992	0.995	0.996	1.002
.15	0.876	0.939	0.975	0.988	0.994	1.003	1.007	1.020
.25	0.833	0.923	0.979	1.000	1.012	1.027	1.033	1.054
.35	0.806	0.920	0.997	1.027	1.044	1.067	1.077	1.106
.45	0.791	0.929	1.028	1.070	1.093	1.126	1.141	1.182
.55	0.784	0.947	1.076	1.134	1.167	1.216	1.238	1.303
.65	0.783	0.976	1.152	1.239	1.293	1.379	1.422	1.561

Table 24. Normalized stress intensity factors calculated at the midsection of an internal planar elliptic crack with d/h=0.20 in a plate under uniform tension N.

K_A/K_o

L_o/h \ a/L_o→	0.5	1.0	2.0	3.0	4.0	7.0	10.0	Plane Strain
.05	0.964	0.967	0.983	0.989	0.991	0.995	0.996	1.003
.15	0.848	0.928	0.974	0.990	0.999	1.011	1.016	1.033
.25	0.790	0.914	0.992	1.022	1.039	1.062	1.073	1.107
.35	0.761	0.933	1.054	1.104	1.133	1.176	1.196	1.258
.45	0.770	1.019	1.202	1.289	1.342	1.424	1.463	1.587
.55	0.896	1.293	1.666	1.863	1.990	2.204	2.316	2.710

K_B/K_o

L_o/h \ a/L_o→	0.5	1.0	2.0	3.0	4.0	7.0	10.0	Plane Strain
.05	0.939	0.968	0.984	0.989	0.992	0.995	0.996	1.003
.15	0.863	0.933	0.974	0.988	0.996	1.006	1.011	1.026
.25	0.818	0.918	0.982	1.006	1.020	1.038	1.046	1.072
.35	0.793	0.918	1.007	1.043	1.063	1.092	1.105	1.144
.45	0.779	0.931	1.049	1.102	1.132	1.178	1.199	1.263
.55	0.770	0.955	1.121	1.204	1.256	1.340	1.382	1.524

Table 25. Normalized stress intensity factors calculated at the midsection of an internal planar elliptic crack with d/h=0.25 in a plate under uniform tension N.

K_A/K_o

L_o/h \ a/L_o →	0.5	1.0	2.0	3.0	4.0	7.0	10.0	Plane Strain
.05	0.927	0.962	0.981	0.988	0.991	0.995	0.997	1.005
.15	0.831	0.922	0.976	0.995	1.006	1.020	1.026	1.048
.25	0.776	0.919	1.013	1.051	1.071	1.101	1.115	1.161
.35	0.768	0.977	1.133	1.201	1.241	1.303	1.333	1.429
.45	0.876	1.228	1.540	1.698	1.798	1.964	2.051	2.353

K_B/K_o

L_o/h \ a/L_o →	0.5	1.0	2.0	3.0	4.0	7.0	10.0	Plane Strain
.05	0.930	0.964	0.982	0.988	0.991	0.995	0.997	1.004
.15	0.847	0.926	0.973	0.991	1.000	1.012	1.017	1.036
.25	0.801	0.913	0.989	1.018	1.034	1.057	1.068	1.102
.35	0.775	0.919	1.026	1.072	1.098	1.138	1.157	1.216
.45	0.758	0.938	1.095	1.172	1.220	1.297	1.336	1.468

Table 26. Normalized stress intensity factors calculated at the midsection of an internal planar elliptic crack with d/h=0.30 in a plate under uniform tension N.

K_A/K_o

L_o/h \ a/L_o→	0.5	1.0	2.0	3.0	4.0	7.0	10.0	Plane Strain
.05	0.917	0.958	0.980	0.987	0.991	0.996	0.998	1.007
.15	0.816	0.921	0.985	1.008	1.021	1.038	1.046	1.073
.25	0.780	0.951	1.070	1.119	1.146	1.187	1.207	1.273
.35	0.869	1.170	1.420	1.537	1.610	1.727	1.787	1.996

K_B/K_o

L_o/h \ a/L_o→	0.5	1.0	2.0	3.0	4.0	7.0	10.0	Plane Strain
.05	0.919	0.959	0.980	0.987	0.991	0.996	0.997	1.006
.15	0.829	0.920	0.976	0.997	1.008	1.023	1.030	1.053
.25	0.783	0.914	1.005	1.042	1.063	1.093	1.108	1.156
.35	0.753	0.927	1.071	1.138	1.178	1.243	1.276	1.387

Table 27. Normalized stress intensity factors calculated at the midsection of an internal planar elliptic crack with d/h=0.05 in a plate under uniform bending M.

K_A/K_o

L_o/h \ a/L_o →	1.0	2.0	3.0	4.0	7.0	10.0	Plane Strain
.05	0.118	0.119	0.120	0.120	0.120	0.120	0.121
.15	0.170	0.173	0.174	0.175	0.176	0.176	0.177
.25	0.217	0.222	0.224	0.225	0.227	0.228	0.230
.35	0.266	0.274	0.278	0.279	0.282	0.283	0.287
.45	0.316	0.329	0.335	0.338	0.342	0.344	0.350
.55	0.371	0.391	0.400	0.405	0.412	0.416	0.426
.65	0.436	0.469	0.484	0.493	0.506	0.513	0.532
.75	0.528	0.586	0.614	0.631	0.659	0.673	0.716
.85	0.753	0.889	0.963	1.013	1.099	1.144	1.313

K_B/K_o

L_o/h \ a/L_o →	1.0	2.0	3.0	4.0	7.0	10.0	Plane Strain
.05	0.073	0.074	0.074	0.074	0.074	0.075	0.075
.15	0.020	0.023	0.024	0.025	0.025	0.026	0.026
.25	-0.032	-0.027	-0.025	-0.024	-0.023	-0.022	-0.021
.35	-0.082	-0.075	-0.073	-0.072	-0.070	-0.069	-0.068
.45	-0.130	-0.123	-0.120	-0.118	-0.116	-0.115	-0.113
.55	-0.178	-0.170	-0.167	-0.165	-0.162	-0.161	-0.159
.65	-0.226	-0.219	-0.215	-0.213	-0.210	-0.209	-0.207
.75	-0.278	-0.272	-0.269	-0.267	-0.264	-0.262	-0.259
.85	-0.339	-0.338	-0.334	-0.331	-0.325	-0.322	-0.311

Table 28. Normalized stress intensity factors calculated at the midsection of an internal planar elliptic crack with d/h=0.10 in a plate under uniform bending M.

K_A/K_o

L_o/h \ a/L_o →	1.0	2.0	3.0	4.0	7.0	10.0	Plane Strain
.05	0.216	0.218	0.219	0.219	0.220	0.220	0.221
.15	0.263	0.270	0.273	0.274	0.276	0.276	0.279
.25	0.308	0.321	0.325	0.328	0.331	0.332	0.337
.35	0.357	0.376	0.383	0.387	0.393	0.395	0.403
.45	0.412	0.440	0.451	0.457	0.467	0.471	0.484
.55	0.477	0.520	0.538	0.549	0.566	0.574	0.598
.65	0.571	0.642	0.676	0.697	0.730	0.746	0.797
.75	0.804	0.959	1.045	1.101	1.199	1.251	1.441

K_B/K_o

L_o/h \ a/L_o →	1.0	2.0	3.0	4.0	7.0	10.0	Plane Strain
.05	0.170	0.172	0.173	0.173	0.174	0.174	0.175
.15	0.114	0.120	0.123	0.124	0.125	0.126	0.128
.25	0.061	0.071	0.075	0.077	0.080	0.081	0.084
.35	0.010	0.024	0.030	0.033	0.037	0.038	0.043
.45	-0.038	-0.020	-0.013	-0.009	-0.004	-0.001	0.005
.55	-0.084	-0.062	-0.053	-0.048	-0.040	-0.037	-0.028
.65	-0.128	-0.102	-0.089	-0.082	-0.071	-0.066	-0.052
.75	-0.171	-0.137	-0.117	-0.105	-0.083	-0.073	-0.037

Table 29. Normalized stress intensity factors calculated at the midsection of an internal planar elliptic crack with d/h=0.15 in a plate under uniform bending M.

K_A/K_o

L_o/h \ $a/L_o \rightarrow$	1.0	2.0	3.0	4.0	7.0	10.0	Plane Strain
.05	0.313	0.317	0.319	0.319	0.320	0.321	0.323
.15	0.355	0.367	0.371	0.373	0.376	0.378	0.382
.25	0.399	0.420	0.428	0.432	0.438	0.440	0.449
.35	0.450	0.482	0.495	0.502	0.512	0.517	0.532
.45	0.514	0.563	0.584	0.596	0.614	0.623	0.650
.55	0.610	0.689	0.727	0.750	0.786	0.804	0.860
.65	0.846	1.015	1.106	1.167	1.270	1.325	1.524

K_B/K_o

L_o/h \ $a/L_o \rightarrow$	1.0	2.0	3.0	4.0	7.0	10.0	Plane Strain
.05	0.266	0.270	0.272	0.273	0.273	0.274	0.275
.15	0.207	0.218	0.221	0.223	0.226	0.227	0.231
.25	0.152	0.169	0.176	0.179	0.184	0.186	0.191
.35	0.101	0.125	0.134	0.139	0.146	0.149	0.158
.45	0.055	0.085	0.098	0.105	0.116	0.120	0.133
.55	0.011	0.051	0.069	0.080	0.096	0.104	0.125
.65	-0.028	0.028	0.058	0.077	0.108	0.123	0.176

Table 30. Normalized stress intensity factors calculated at the midsection of an internal planar elliptic crack with d/h=0.20 in a plate under uniform bending M.

K_A/K_o

L_o/h \ $a/L_o \rightarrow$	1.0	2.0	3.0	4.0	7.0	10.0	Plane Strain
.05	0.410	0.417	0.419	0.420	0.421	0.422	0.425
.15	0.445	0.464	0.471	0.474	0.479	0.481	0.488
.25	0.490	0.522	0.534	0.541	0.551	0.555	0.569
.35	0.549	0.600	0.621	0.633	0.651	0.660	0.687
.45	0.642	0.725	0.764	0.787	0.823	0.841	0.897
.55	0.875	1.050	1.142	1.202	1.303	1.357	1.549

K_B/K_o

L_o/h \ $a/L_o \rightarrow$	1.0	2.0	3.0	4.0	7.0	10.0	Plane Strain
.05	0.362	0.368	0.370	0.372	0.373	0.373	0.376
.15	0.298	0.315	0.321	0.324	0.328	0.329	0.336
.25	0.242	0.268	0.278	0.283	0.291	0.294	0.304
.35	0.193	0.229	0.244	0.252	0.264	0.269	0.285
.45	0.148	0.197	0.219	0.232	0.252	0.261	0.289
.55	0.109	0.181	0.218	0.242	0.280	0.299	0.365

Table 31. Normalized stress intensity factors calculated at the midsection of an internal planar elliptic crack with d/h=0.25 in a plate under uniform bending M.

K_A/K_o

L_o/h \ a/L_o →	1.0	2.0	3.0	4.0	7.0	10.0	Plane Strain
.05	0.506	0.516	0.519	0.520	0.523	0.523	0.527
.15	0.535	0.563	0.573	0.578	0.585	0.589	0.599
.25	0.585	0.633	0.652	0.662	0.677	0.685	0.708
.35	0.670	0.751	0.787	0.808	0.840	0.856	0.907
.45	0.895	1.066	1.152	1.206	1.298	1.346	1.515

K_B/K_o

L_o/h \ a/L_o →	1.0	2.0	3.0	4.0	7.0	10.0	Plane Strain
.05	0.457	0.466	0.469	0.471	0.473	0.473	0.477
.15	0.388	0.412	0.421	0.425	0.431	0.434	0.443
.25	0.332	0.370	0.385	0.393	0.405	0.410	0.427
.35	0.285	0.340	0.363	0.377	0.398	0.407	0.438
.45	0.305	0.332	0.369	0.395	0.437	0.459	0.513

Table 32. Normalized stress intensity factors calculated at the midsection of an internal planar elliptic crack with d/h=0.30 in a plate under uniform bending M.

K_A/K_o

L_o/h \ a/L_o →	1.0	2.0	3.0	4.0	7.0	10.0	Plane Strain
.05	0.600	0.614	0.618	0.621	0.624	0.625	0.630
.15	0.627	0.666	0.680	0.688	0.698	0.703	0.720
.25	0.698	0.771	0.801	0.817	0.842	0.855	0.895
.35	0.910	1.067	1.141	1.187	1.261	1.300	1.432

K_B/K_o

L_o/h \ a/L_o →	1.0	2.0	3.0	4.0	7.0	10.0	Plane Strain
.05	0.550	0.563	0.567	0.570	0.572	0.574	0.579
.15	0.477	0.511	0.524	0.530	0.539	0.543	0.557
.25	0.423	0.479	0.501	0.514	0.533	0.542	0.570
.35	0.381	0.471	0.513	0.538	0.579	0.600	0.669

Table 33. Normalized stress intensity factors calculated at the midsection of two opposite planar elliptic edge cracks in a plate under uniform tension N.

L_o/h \ a/L_o →	1.0	2.0	3.0	4.0	10.0	100.0	Plane Strain
0.1	1.060	1.089	1.099	1.104	1.113	1.119	1.123
0.2	1.009	1.062	1.081	1.091	1.109	1.121	1.125
0.3	0.966	1.028	1.065	1.079	1.106	1.124	1.129
0.4	0.929	1.019	1.053	1.072	1.108	1.131	1.137
0.5	0.902	1.008	1.050	1.073	1.118	1.148	1.155
0.6	0.902	1.038	1.080	1.108	1.165	1.203	1.212
0.7	0.929	1.082	1.149	1.186	1.262	1.315	1.325
0.8	0.997	1.195	1.284	1.336	1.445	1.524	1.539

Table 34. Maximum normalized stress intensity factors for two planar elliptic edge cracks in a plate under pure tension N.

L_o/h	a/L_o	b/a → 0.1	1.0	4.0	20.0	Single Crack
0.1	2	0.996	0.986	0.982	0.981	0.981
0.1	4	1.072	1.065	1.062	1.062	1.062
0.1	10	1.127	1.122	1.121	1.120	1.120
0.2	2	0.979	0.959	0.951	0.949	0.949
0.2	4	1.107	1.090	1.084	1.082	1.082
0.2	10	1.221	1.210	1.207	1.206	1.206
0.3	2	1.007	0.975	0.963	0.961	0.961
0.3	4	1.189	1.160	1.151	1.149	1.149
0.3	10	1.382	1.364	1.359	1.358	1.358
0.4	2	1.051	1.006	0.991	0.989	0.989
0.4	4	1.299	1.255	1.243	1.240	1.240
0.4	10	1.600	1.571	1.563	1.562	1.562
0.5	2	1.106	1.048	1.032	1.030	1.030
0.5	4	1.430	1.370	1.354	1.352	1.352
0.5	10	1.879	1.836	1.824	1.822	1.821
0.6	2	1.230	1.096	1.080	1.077	1.077
0.6	4	1.568	1.491	1.472	1.469	1.469
0.6	10	2.208	2.141	2.124	2.121	2.121
0.7	2	1.370	1.120	1.100	1.097	1.097
0.7	4	1.694	1.575	1.553	1.550	1.550
0.7	10	2.532	2.434	2.409	2.405	2.405

Table 35. Maximum normalized stress intensity factors for two planar elliptic edge cracks in a plate under uniform bending M.

L_o/h	a/L_o	b/a ⟶ 0.1	1.0	4.0	20.0	Single Crack
0.1	2	0.874	0.864	0.861	0.860	0.860
0.1	4	0.943	0.936	0.934	0.933	0.933
0.1	10	0.992	0.988	0.987	0.986	0.986
0.2	2	0.766	0.728	0.719	0.718	0.718
0.2	4	0.847	0.830	0.825	0.824	0.824
0.2	10	0.940	0.930	0.927	0.927	0.927
0.3	2	0.751	0.665	0.651	0.650	0.650
0.3	4	0.803	0.755	0.745	0.744	0.744
0.3	10	0.915	0.900	0.896	0.896	0.895
0.4	2	0.792	0.677	0.659	0.658	0.656
0.4	4	0.801	0.726	0.713	0.711	0.711
0.4	10	0.923	0.902	0.896	0.895	0.895
0.5	2	0.826	0.684	0.663	0.661	0.659
0.5	4	0.834	0.719	0.703	0.701	0.700
0.5	10	0.950	0.910	0.902	0.901	0.901
0.6	2	0.855	0.686	0.662	0.660	0.659
0.6	4	0.909	0.743	0.724	0.722	0.721
0.6	10	0.995	0.925	0.912	0.910	0.910
0.7	2	0.874	0.683	0.658	0.655	0.654
0.7	4	0.989	0.784	0.761	0.759	0.757
0.7	10	1.064	0.956	0.939	0.937	0.936

Table 36. Normalized stress intensity factors calculated at the midsection of symmetrically located(d=0) two identical planar internal elliptic cracks in a plate under uniform tension N.

L_o/h	a/L_o	b/a → 0.1	1.0	4.0	20.0	Single Crack
0.1	2	0.977	0.976	0.976	0.976	0.967
0.1	4	0.987	0.987	0.987	0.986	0.987
0.1	10	0.994	0.993	0.993	0.993	0.993
0.2	2	0.975	0.972	0.971	0.971	0.971
0.2	4	0.995	0.994	0.993	0.993	0.993
0.2	10	1.008	1.007	1.007	1.007	1.007
0.3	2	0.980	0.980	0.979	0.979	0.979
0.3	4	1.015	1.013	1.012	1.012	1.012
0.3	10	1.035	1.034	1.034	1.034	1.034
0.4	2	1.007	1.002	1.000	1.000	1.000
0.4	4	1.051	1.048	1.047	1.047	1.047
0.4	10	1.080	1.078	1.078	1.078	1.078
0.5	2	1.046	1.039	1.037	1.036	1.036
0.5	4	1.106	1.102	1.101	1.101	1.101
0.5	10	1.147	1.145	1.145	1.145	1.145
0.6	2	1.108	1.098	1.095	1.095	1.095
0.6	4	1.190	1.185	1.183	1.183	1.183
0.6	10	1.248	1.246	1.245	1.245	1.245
0.7	2	1.205	1.192	1.188	1.187	1.187
0.7	4	1.321	1.313	1.311	1.310	1.310
0.7	10	1.407	1.404	1.403	1.403	1.403
0.8	2	1.367	1.348	1.342	1.341	1.341
0.8	4	1.541	1.529	1.526	1.525	1.525
0.8	10	1.681	1.676	1.674	1.674	1.674
0.9	2	1.703	1.672	1.662	1.661	1.661
0.9	4	2.007	1.988	1.982	1.981	1.981
0.9	10	2.285	2.275	2.272	2.272	

Table 37. Normalized stress intensity factors calculated at the midsection of two identical planar internal elliptic cracks in a plate under uniform tension N.

			K_A/K_o			
			b/a → 0.1	1.0	4.0	20.0
d	L_o/h	a/L_o				
0.1	0.1	2	0.957	0.821	0.981	0.979
0.1	0.1	4	1.002	0.994	0.992	0.991
0.1	0.1	10	1.000	0.999	0.999	0.999
0.1	0.2	2	1.027	0.986	0.977	0.976
0.1	0.2	4	1.005	1.002	1.001	1.001
0.1	0.2	10	1.018	1.018	1.018	1.018
0.1	0.3	2	1.012	0.995	0.990	0.989
0.1	0.3	4	1.034	1.032	1.031	1.031
0.1	0.3	10				
0.1	0.35	2	1.021	1.010	1.005	1.004
0.1	0.35	4	1.058	1.056	1.055	1.055
0.1	0.35	10				
0.2	0.1	2	0.947	0.783	0.979	0.976
0.2	0.1	4	1.006	0.995	0.992	0.992
0.2	0.1	10	1.003	1.002	1.002	1.002
0.2	0.2	2	1.052	0.993	0.981	0.979
0.2	0.2	4	1.020	1.016	1.014	1.014
0.2	0.2	10	1.039	1.038	1.038	1.038
0.2	0.25	2	1.056	1.003	0.994	0.992
0.2	0.25	4	1.044	1.040	1.040	1.039
0.2	0.25	10	1.073	1.073	1.073	1.073
0.3	0.1	2	0.933	0.760	0.980	0.975
0.3	0.1	4	1.018	1.003	0.999	0.998
0.3	0.1	10	1.014	1.013	1.013	1.013
0.3	0.15	2	0.814	0.985	0.988	0.985
0.3	0.15	4	1.033	1.024	1.022	1.021
0.3	0.15	10	1.047	1.046	1.046	1.046

Table 37- Cont.

K_B/K_o

d	L_o/h	a/L_o	b/a → 0.1	1.0	4.0	20.0
0.1	0.1	2	0.959	0.830	0.982	0.979
0.1	0.1	4	1.002	0.993	0.991	0.991
0.1	0.1	10	0.999	0.999	0.999	0.999
0.1	0.2	2	1.020	0.984	0.978	0.976
0.1	0.2	4	1.002	1.000	0.999	0.999
0.1	0.2	10	1.014	1.014	1.014	1.014
0.1	0.3	2	1.004	0.989	0.985	0.984
0.1	0.3	4	1.021	1.020	1.019	1.019
0.1	0.3	10				
0.1	0.35	2	1.006	0.997	0.993	0.993
0.1	0.35	4	1.036	1.035	1.034	1.034
0.1	0.35	10				
0.2	0.1	2	0.950	0.799	0.979	0.976
0.2	0.1	4	1.004	0.994	0.992	0.991
0.2	0.1	10	1.001	1.001	1.001	1.001
0.2	0.2	2	1.038	0.987	0.977	0.976
0.2	0.2	4	1.010	1.007	1.006	1.005
0.2	0.2	10	1.026	1.026	1.026	1.026
0.2	0.25	2	1.034	0.990	0.983	0.982
0.2	0.25	4	1.023	1.021	1.020	1.019
0.2	0.25	10	1.046	1.046	1.046	1.046
0.3	0.1	2	0.935	0.778	0.978	0.974
0.3	0.1	4	1.013	0.999	0.996	0.995
0.3	0.1	10	1.009	1.009	1.008	1.008
0.3	0.15	2	0.829	0.977	0.979	0.977
0.3	0.15	4	1.019	1.011	1.008	1.008
0.3	0.15	10	1.030	1.030	1.030	1.030

Table 38. Normalized stress intensity factors calculated at the midsection of three identical planar internal elliptic cracks in a plate under uniform tension N.

K_A/K_o for the middle crack

d	L_o/h	a/L_o	b/a → 0.1	1.0	4.0	20.0
0.1	0.1	2	0.983	0.981	0.979	0.979
0.1	0.1	4	0.994	0.992	0.992	0.991
0.1	0.2	2	0.985	0.980	0.977	0.976
0.1	0.2	4	1.007	1.004	1.002	1.001
0.1	0.3	2	1.006	0.997	0.991	0.989
0.1	0.3	4	1.040	1.035	1.032	1.031
0.2	0.1	2	0.981	0.978	0.976	0.975
0.2	0.1	4	0.995	0.994	0.992	0.992
0.2	0.2	2	0.993	0.986	0.981	0.979
0.2	0.2	4	1.023	1.018	1.015	1.014
0.3	0.1	2	0.983	0.979	0.976	0.975
0.3	0.1	4	1.003	1.001	0.999	0.998

K_B/K_o for the middle crack

0.1	0.1	2	0.984	0.981	0.980	0.979
0.1	0.1	4	0.993	0.992	0.991	0.991
0.1	0.2	2	0.984	0.980	0.977	0.976
0.1	0.2	4	1.003	1.001	0.999	0.999
0.1	0.3	2	0.997	0.990	0.986	0.984
0.1	0.3	4	1.026	1.022	1.020	1.019
0.2	0.1	2	0.981	0.978	0.977	0.976
0.2	0.1	4	0.994	0.993	0.992	0.991
0.2	0.2	2	0.987	0.981	0.977	0.976
0.2	0.2	4	1.012	1.009	1.006	1.005
0.3	0.1	2	0.981	0.977	0.975	0.974
0.3	0.1	4	0.999	0.997	0.996	0.995

Table 38-Cont.

K_A/K_o for outer crack

d	L_o/h	a/L_o	b/a ⟶ 0.1	1.0	4.0	20.0
0.1	0.1	2	0.982	0.980	0.979	0.979
0.1	0.1	4	0.993	0.992	0.991	0.991
0.1	0.2	2	0.982	0.978	0.976	0.976
0.1	0.2	4	1.005	1.003	1.002	1.001
0.1	0.3	2	0.999	0.994	0.991	0.989
0.1	0.3	4	1.037	1.034	1.032	1.031
0.2	0.1	2	0.979	0.977	0.976	0.975
0.2	0.1	4	0.994	0.993	0.992	0.992
0.2	0.2	2	0.988	0.983	0.980	0.979
0.2	0.2	4	1.019	1.016	1.014	1.014
0.3	0.1	2	0.980	0.978	0.976	0.975
0.3	0.1	4	1.001	1.000	0.999	0.998

K_B/K_o for outer crack

0.1	0.1	2	0.982	0.980	0.980	0.979
0.1	0.1	4	0.993	0.992	0.991	0.991
0.1	0.2	2	0.981	0.978	0.976	0.976
0.1	0.2	4	1.002	1.000	0.999	0.999
0.1	0.3	2	0.992	0.988	0.985	0.984
0.1	0.3	4	1.023	1.021	1.020	1.019
0.2	0.1	2	0.979	0.978	0.976	0.976
0.2	0.1	4	0.993	0.992	0.991	0.991
0.2	0.2	2	0.983	0.979	0.977	0.976
0.2	0.2	4	1.010	1.007	1.006	1.005
0.3	0.1	2	0.978	0.976	0.974	0.974
0.3	0.1	4	0.998	0.996	0.995	0.995

Table 39. Normalized stress intensity factors on the crack front for an internal elliptic crack with $d/h=0.20$, $L_o/h=0.45$, $a/L_o=4$.

x	$(K_A/K_o)_N$	$(K_B/K_o)_N$	$(K_B/K_o)_M$	$(K_B/K_o)_M$
0.99	0.426	0.411	0.186	0.151
0.90	0.723	0.707	0.357	0.218
0.80	0.865	0.831	0.454	0.229
0.70	0.974	0.916	0.531	0.233
0.60	1.065	0.980	0.595	0.233
0.50	1.143	1.028	0.649	0.233
0.40	1.211	1.068	0.697	0.233
0.30	1.266	1.096	0.735	0.233
0.20	1.307	1.116	0.763	0.233
0.10	1.333	1.128	0.781	0.233
0.00	1.342	1.132	0.787	0.232

Table 40. Normalized stress intensity factors on the crack front for an internal elliptic crack with d/h=0.10, L_o/h=0.45, a/L_o=4.

x	$(K_A/K_o)_N$	$(K_B/K_o)_N$	$(K_B/K_o)_M$	$(K_B/K_o)_M$
0.99	0.411	0.393	0.097	0.065
0.90	0.692	0.686	0.205	0.072
0.80	0.816	0.804	0.269	0.057
0.70	0.902	0.883	0.318	0.041
0.60	0.967	0.941	0.357	0.028
0.50	1.018	0.984	0.388	0.016
0.40	1.061	1.019	0.414	0.007
0.30	1.092	1.044	0.433	0.000
0.20	1.114	1.061	0.446	-0.005
0.10	1.128	1.072	0.455	-0.008
0.00	1.132	1.075	0.457	-0.009

Table 41. Normalized stress intensity factors on the crack front for an elliptic edge crack with $L_o/h=0.45$, $a/L_o=4$.

x	(K_N/K_o)	(K_M/K_o)
0.99	0.762	0.646
0.90	0.920	0.696
0.80	1.027	0.711
0.70	1.084	0.701
0.60	1.130	0.695
0.50	1.166	0.689
0.40	1.197	0.686
0.30	1.214	0.680
0.20	1.227	0.676
0.10	1.237	0.675
0.00	1.240	0.675

F I G U R E S

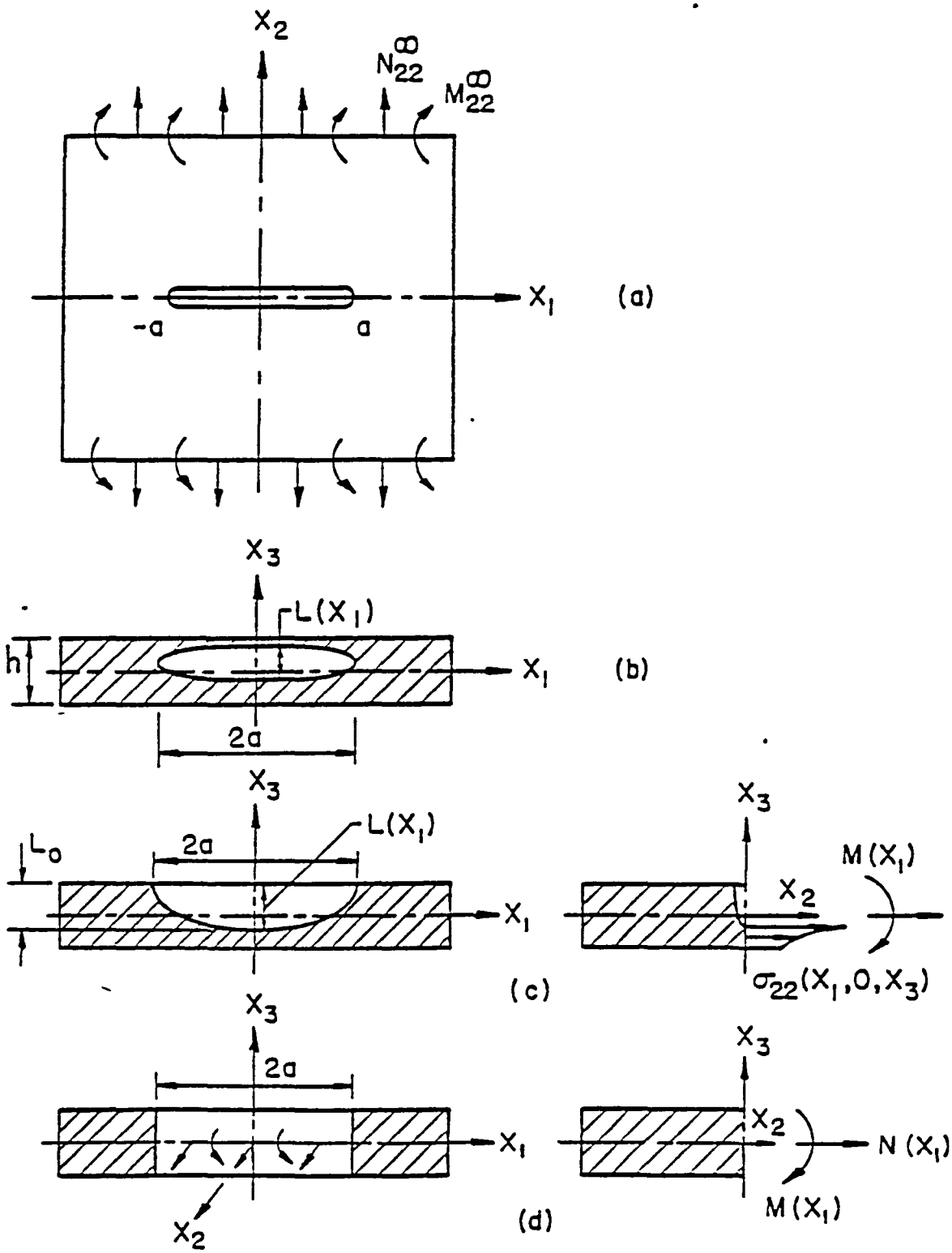

Figure 1. Notation for the part-through crack problem.

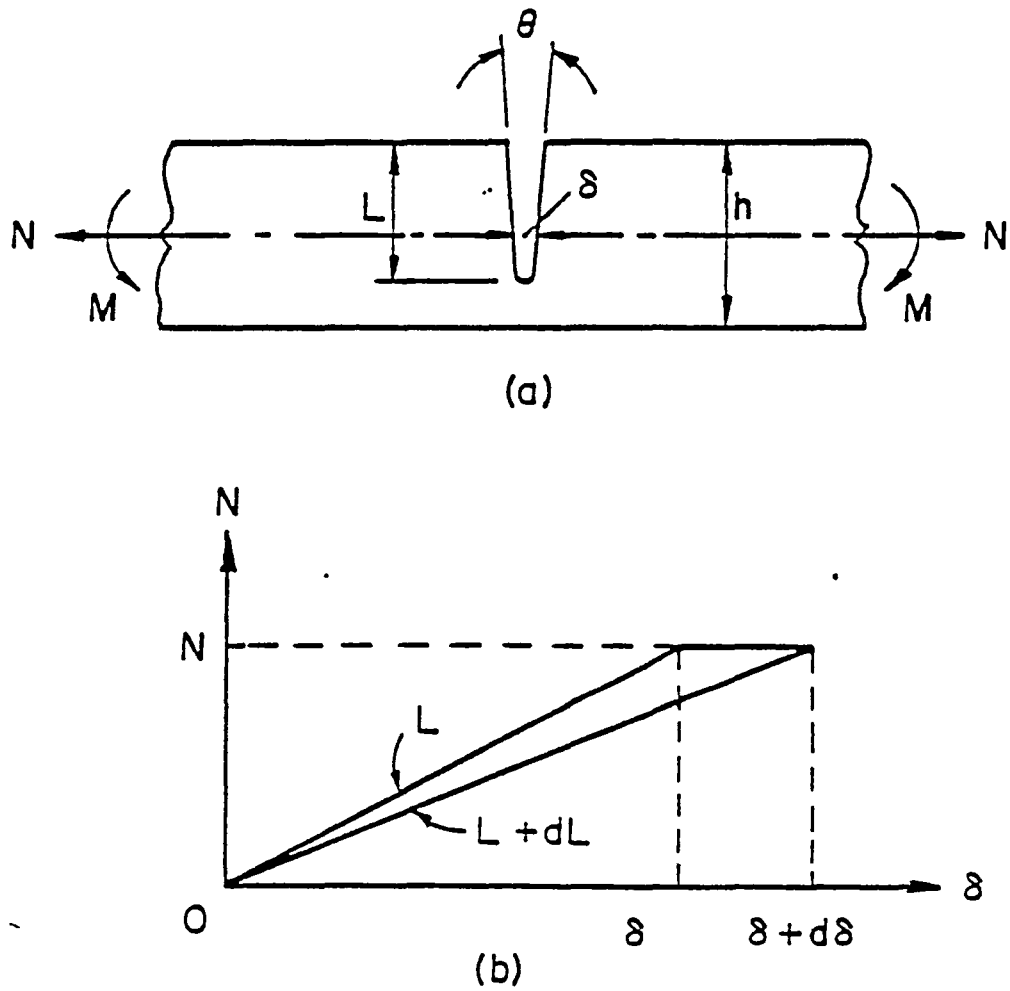

Figure 2. Notation for the related plane strain problem.

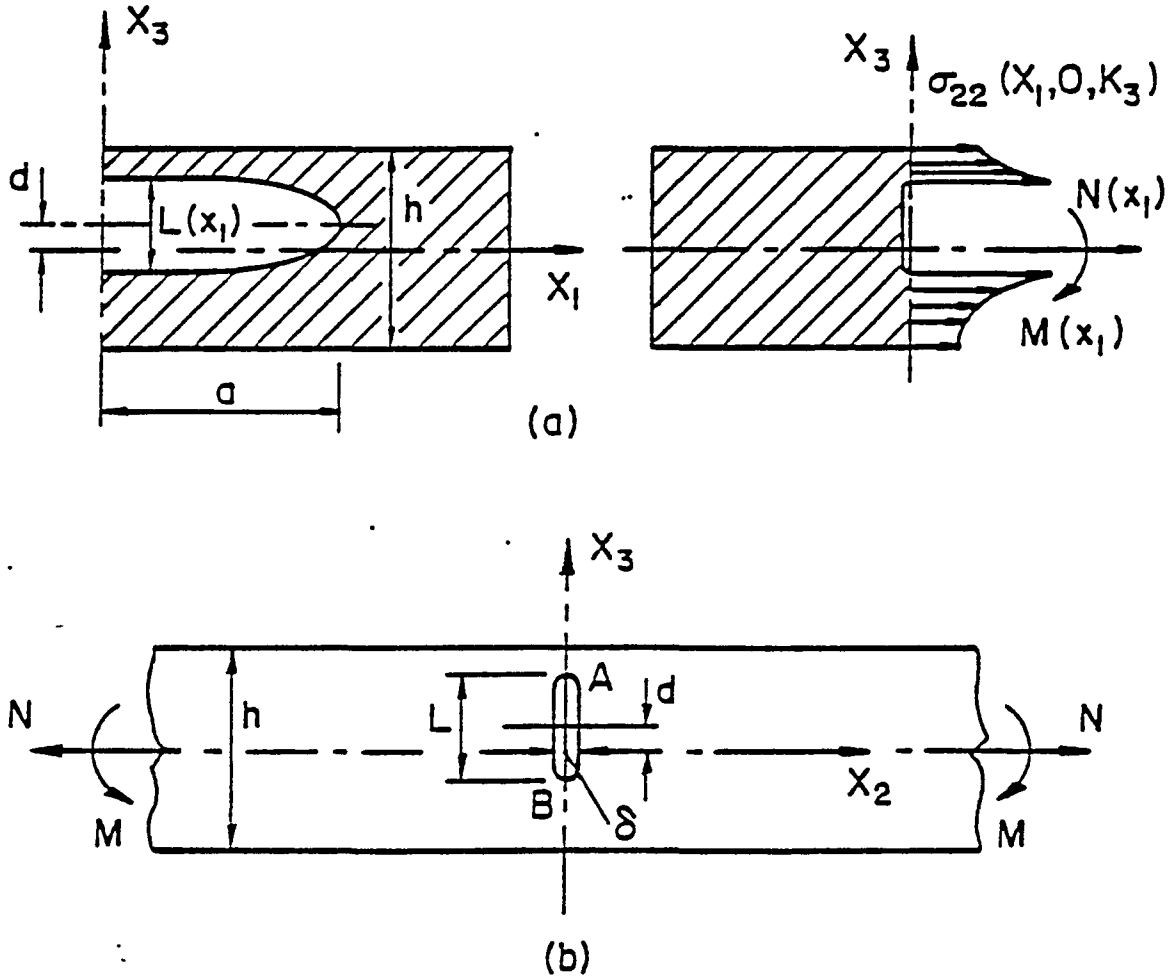

Figure 3. Geometry and notation for an internal crack.

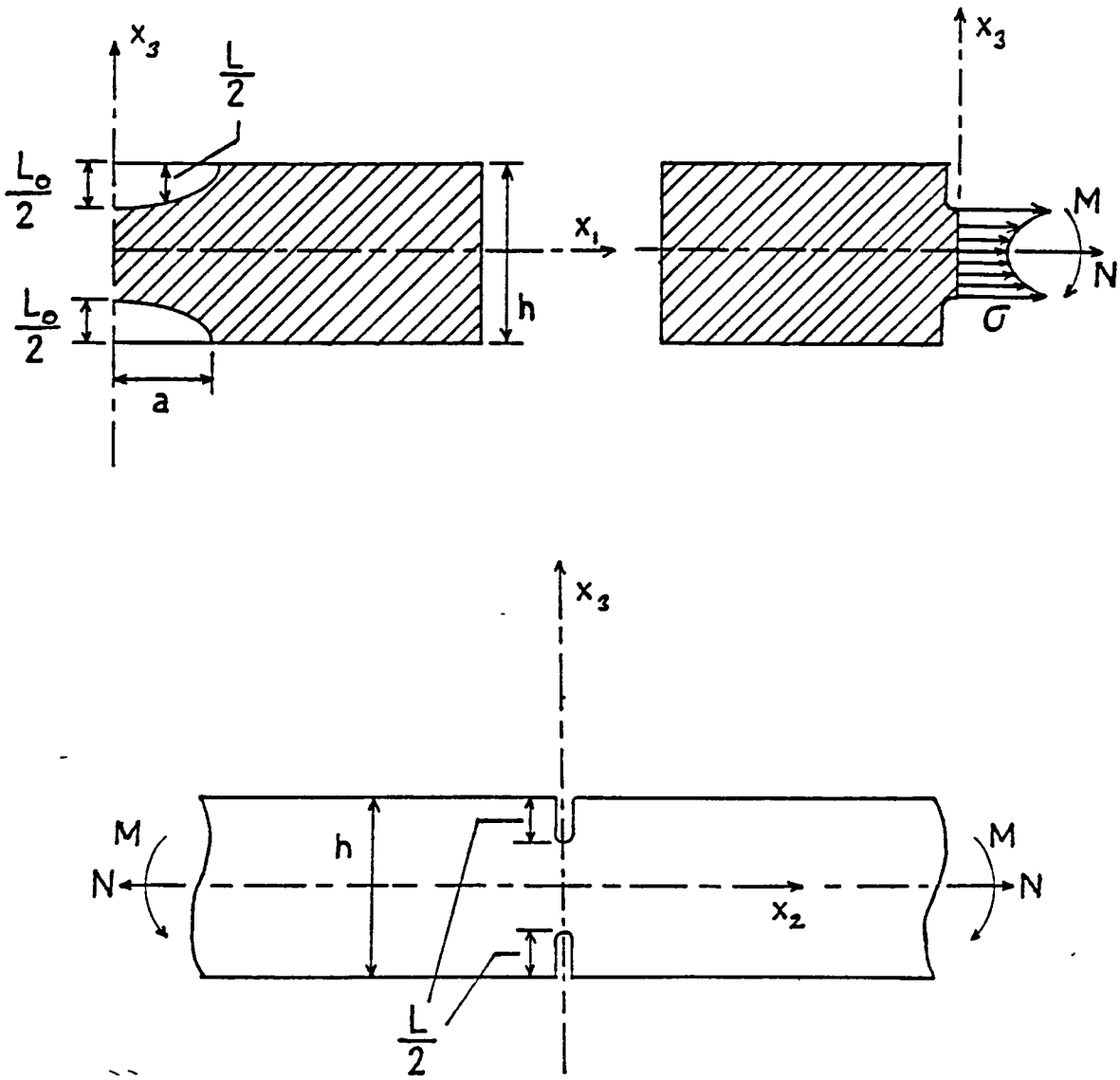

Figure 4. Geometry and notation for two opposite elliptic edge cracks.

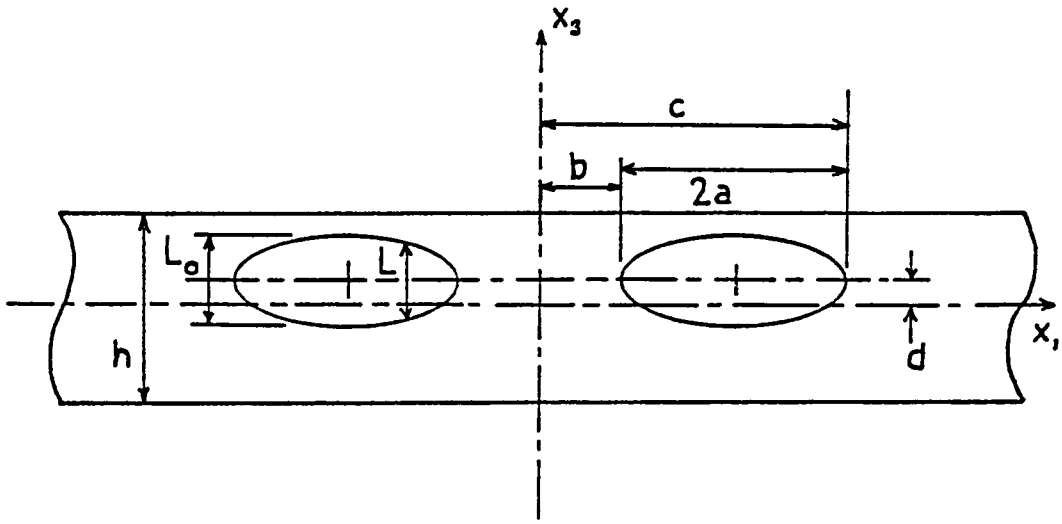

Figure 5. Geometry and notation for two identical cracks.

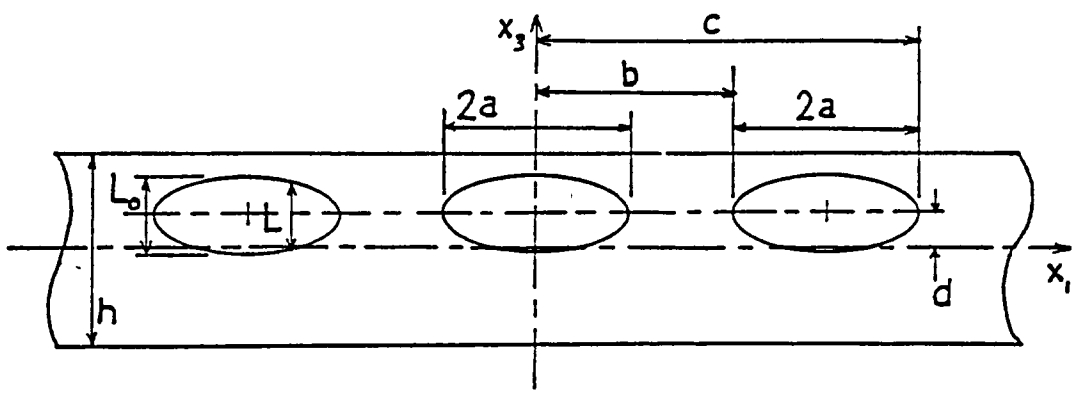

Figure 6. Geometry and notation for three identical cracks.

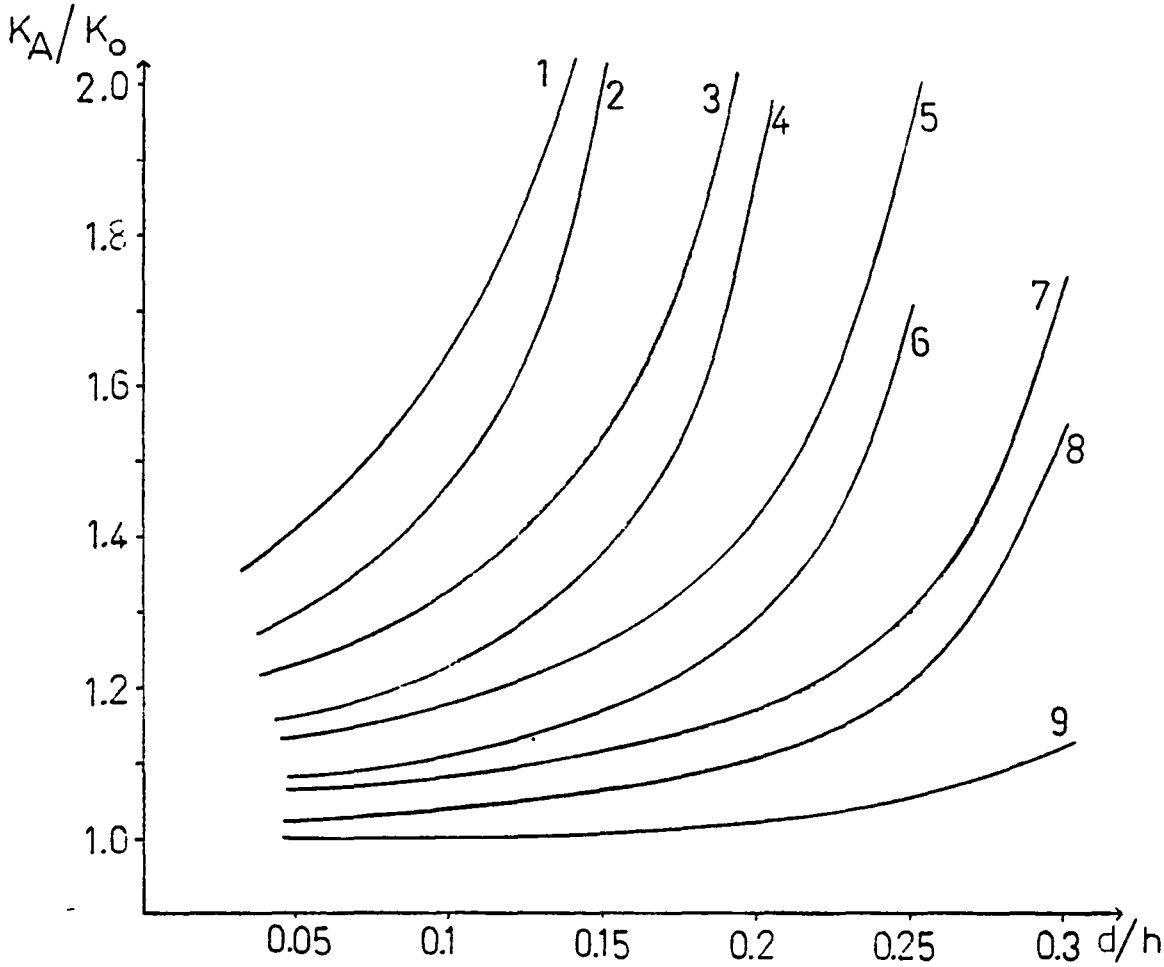

1: $L_o/h=0.65$, $a/L_o=7$,
2: $L_o/h=0.65$, $a/L_o=3$,
3: $L_o/h=0.55$, $a/L_o=7$,
4: $L_o/h=0.55$, $a/L_o=3$,
5: $L_o/h=0.45$, $a/L_o=7$,
6: $L_o/h=0.45$, $a/L_o=3$,
7: $L_o/h=0.35$, $a/L_o=7$,
8: $L_o/h=0.35$, $a/L_o=3$,
9: $L_o/h=0.25$, $a/L_o=3$.

Figure 7. Effect of d/h ratio on the normalized stress intensity factors calculated at the midsection of various internal elliptic cracks under pure tension.

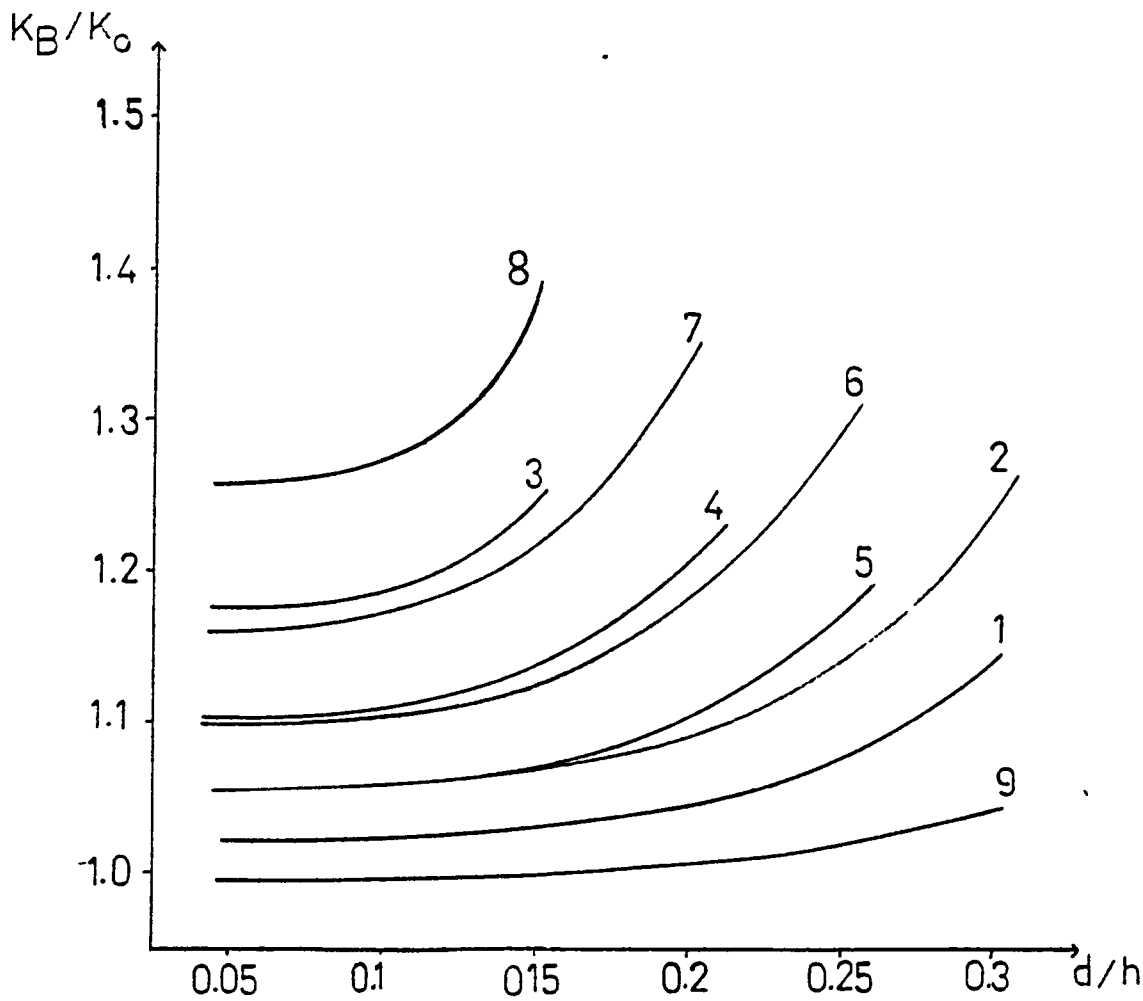

1: $L_o/h=0.35$, $a/L_o=3$,
2: $L_o/h=0.35$, $a/L_o=7$,
3: $L_o/h=0.65$, $a/L_o=3$,
4: $L_o/h=0.55$, $a/L_o=3$,
5: $L_o/h=0.45$, $a/L_o=3$,
6: $L_o/h=0.45$, $a/L_o=7$,
7: $L_o/h=0.55$, $a/L_o=7$,
8: $L_o/h=0.65$, $a/L_o=7$,
9: $L_o/h=0.25$, $a/L_o=3$.

Figure 8. Effect of d/h ratio on the normalized stress intensity factors calculated at the midsection of various internal elliptic cracks under pure tension.

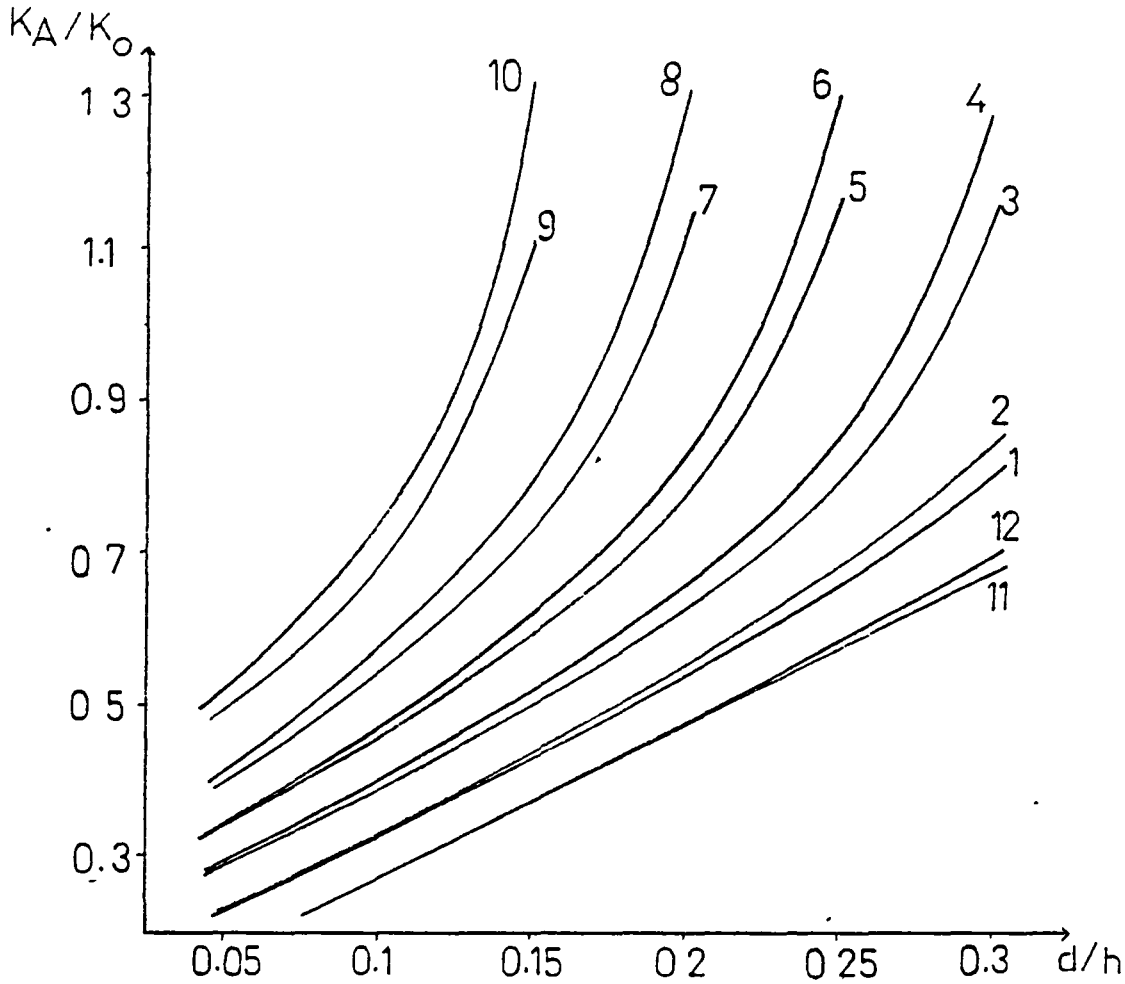

1: $L_o/h=0.25$, $a/L_o=3$,
2: $L_o/h=0.25$, $a/L_o=7$,
3: $L_o/h=0.35$, $a/L_o=3$,
4: $L_o/h=0.35$, $a/L_o=7$,
5: $L_o/h=0.45$, $a/L_o=3$,
6: $L_o/h=0.45$, $a/L_o=7$,
7: $L_o/h=0.55$, $a/L_o=3$,
8: $L_o/h=0.55$, $a/L_o=7$,
9: $L_o/h=0.65$, $a/L_o=3$,
10: $L_o/h=0.65$, $a/L_o=7$,
11: $L_o/h=0.15$, $a/L_o=3$,
12: $L_o/h=0.15$, $a/L_o=7$.

Figure 9. Effect of d/h ratio on the normalized stress intensity factors calculated at the midsection of various internal elliptic cracks under pure bending.

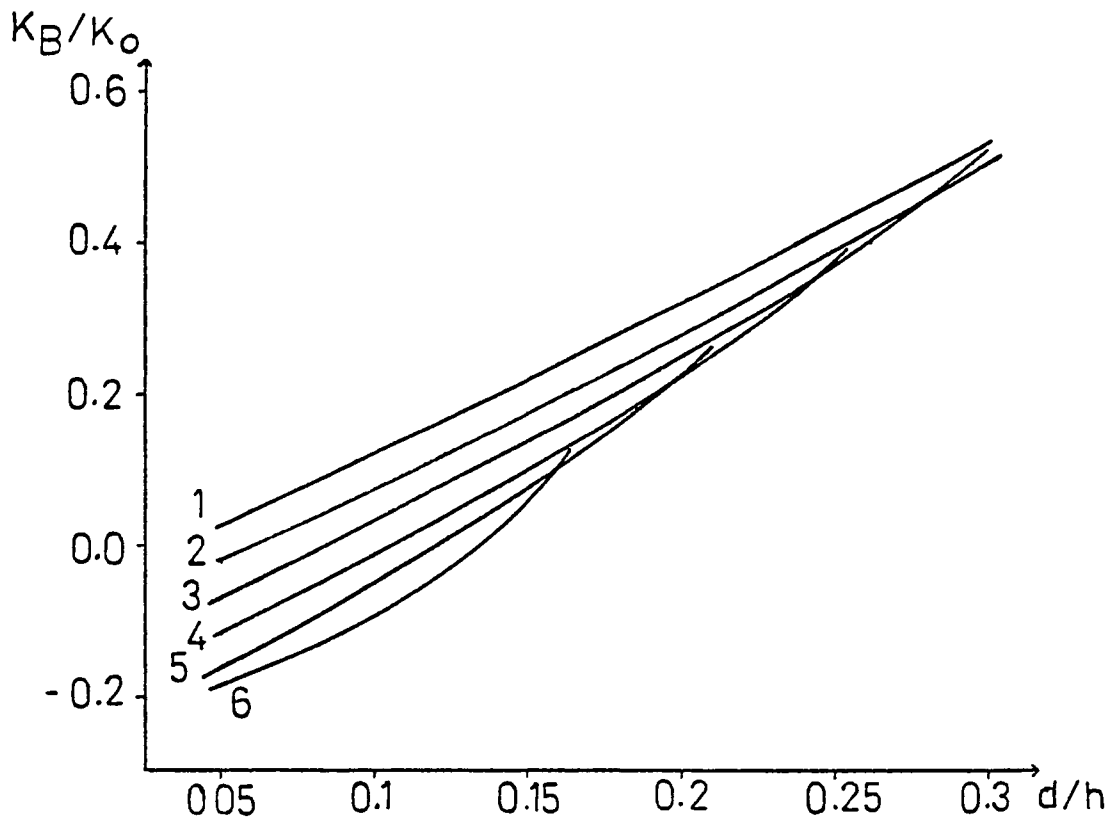

1: $L_o/h=0.15$, $a/L_o=3$,
2: $L_o/h=0.25$, $a/L_o=3$,
3: $L_o/h=0.35$, $a/L_o=3$,
4: $L_o/h=0.45$, $a/L_o=3$,
5: $L_o/h=0.55$, $a/L_o=3$,
6: $L_o/h=0.65$, $a/L_o=3$,

Figure 10. Effect of d/h ratio on the normalized stress intensity factors calculated at the midsection of various internal elliptic cracks under pure bending.

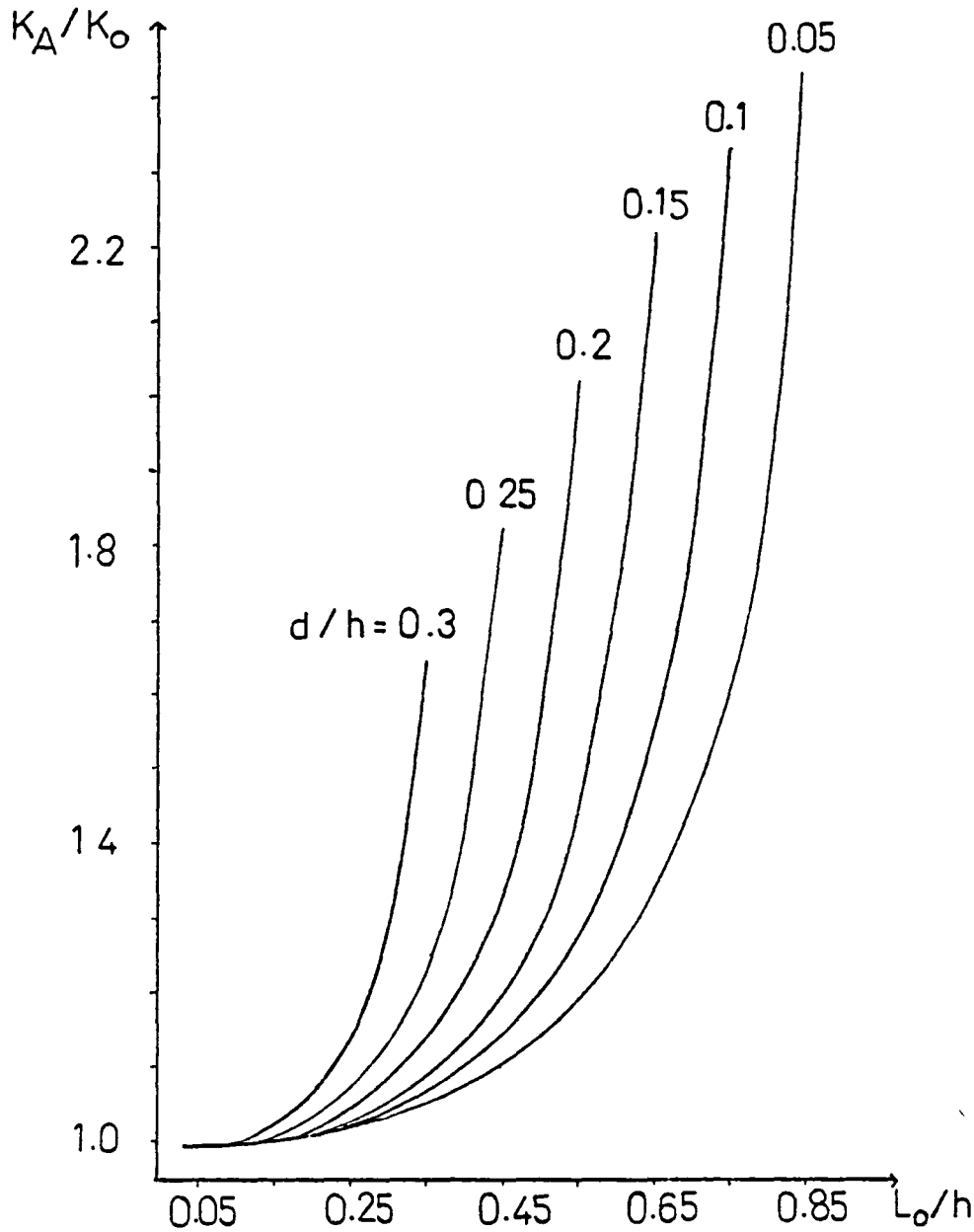

Figure 11. Effect of L_o/h ratio on the normalized stress intensity factors calculated at the midsection of internal elliptic cracks with $a/L_o=4$ and different d/h ratios under pure tension.

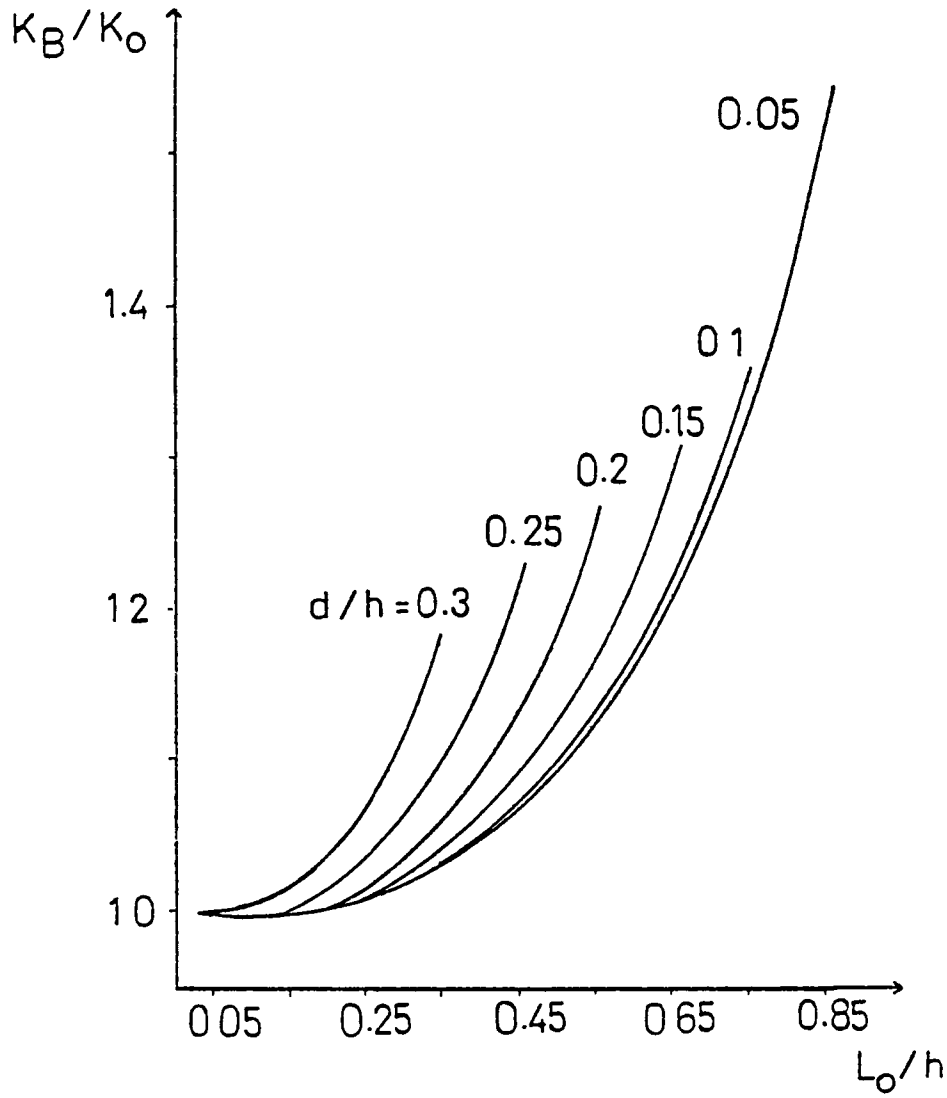

Figure 12. Effect of L_o/h ratio on the normalized stress intensity factors calculated at the midsection of internal elliptic cracks with $a/L_o=4$ and different d/h ratios under pure tension.

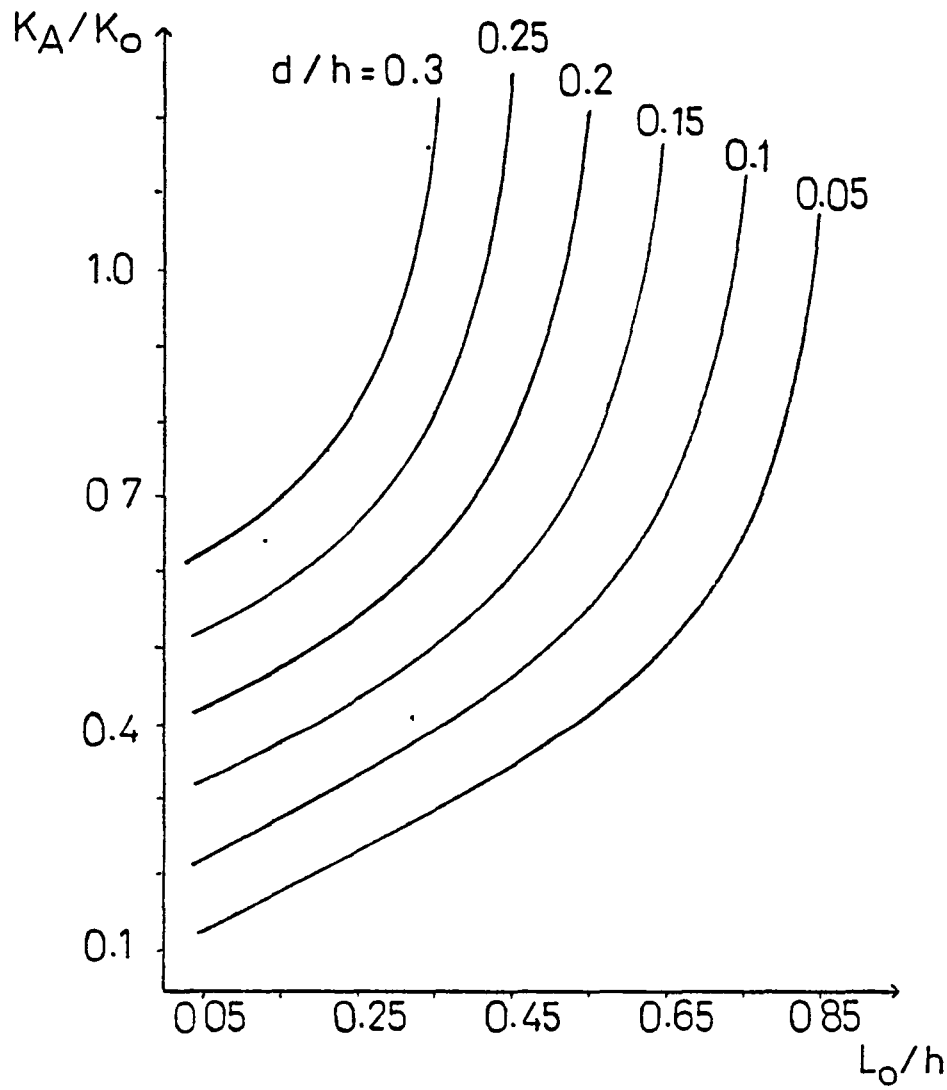

Figure 13. Effect of L_o/h ratio on the normalized stress intensity factors calculated at the midsection of internal elliptic cracks with $a/L_o=4$ and different d/h ratios under pure bending.

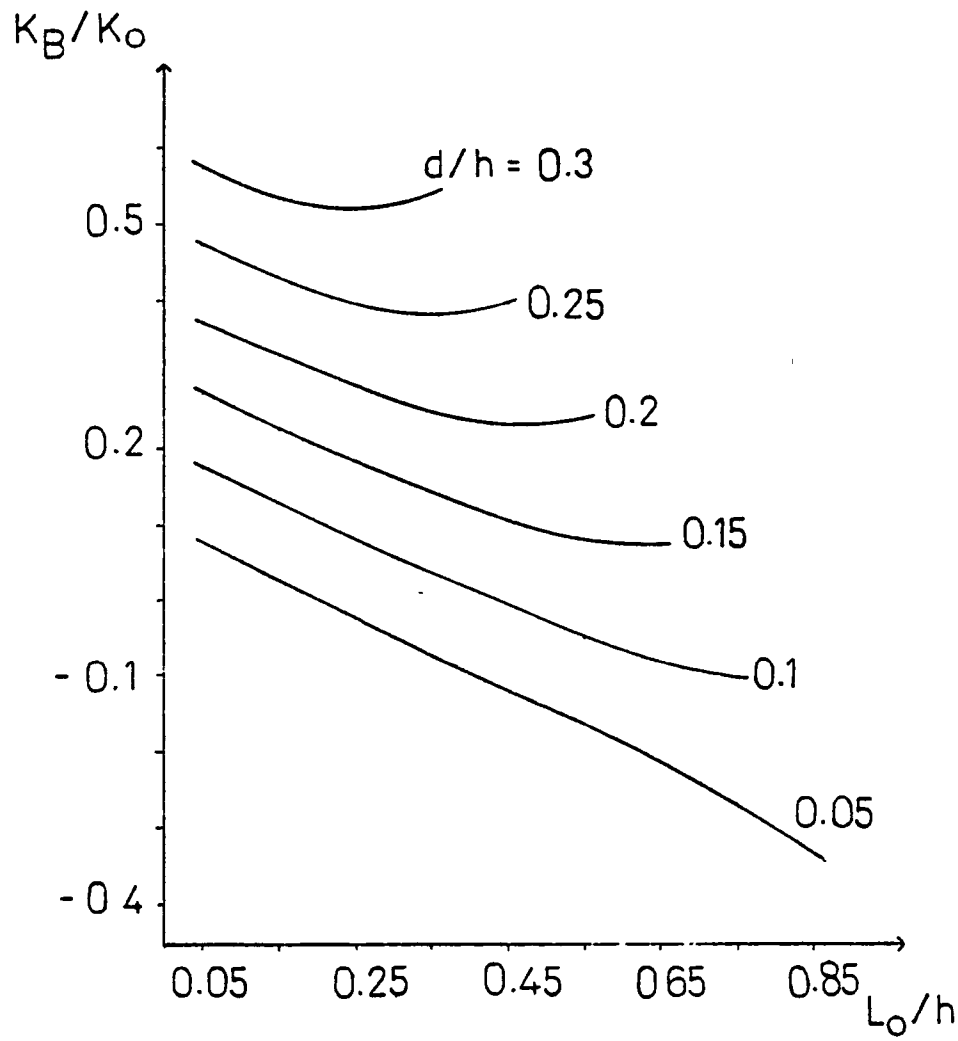

Figure 14. Effect of L_o/h ratio on the normalized stress intensity factors calculated at the midsection of internal elliptic cracks with $a/L_o=4$ and different d/h ratios under pure bending.

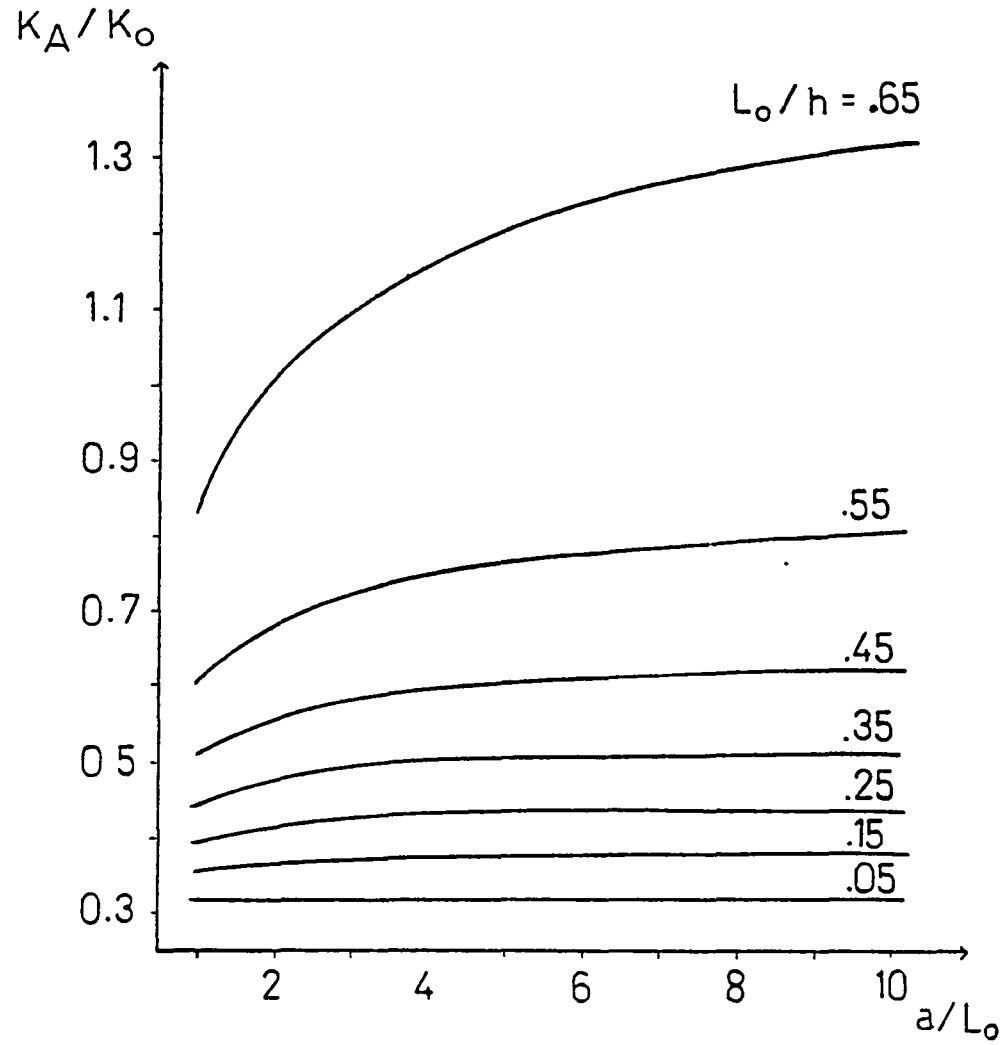

Figure 15. Effect of a/L_o ratio on the normalized stress intensity factors calculated at the midsection of internal elliptic cracks with d/h=0.15 and different L_o/h ratios under pure bending.

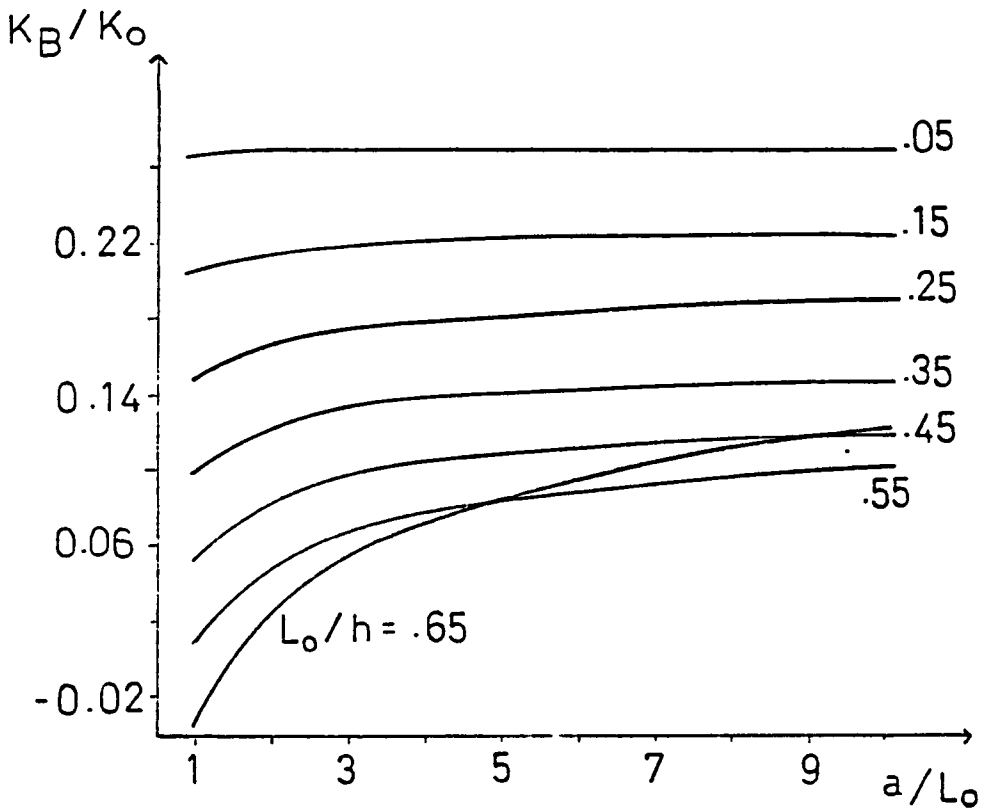

Figure 16. Effect of a/L_o ratio on the normalized stress intensity factors calculated at the midsection of internal elliptic cracks with d/h=0.15 and different L_o/h ratios under pure bending.

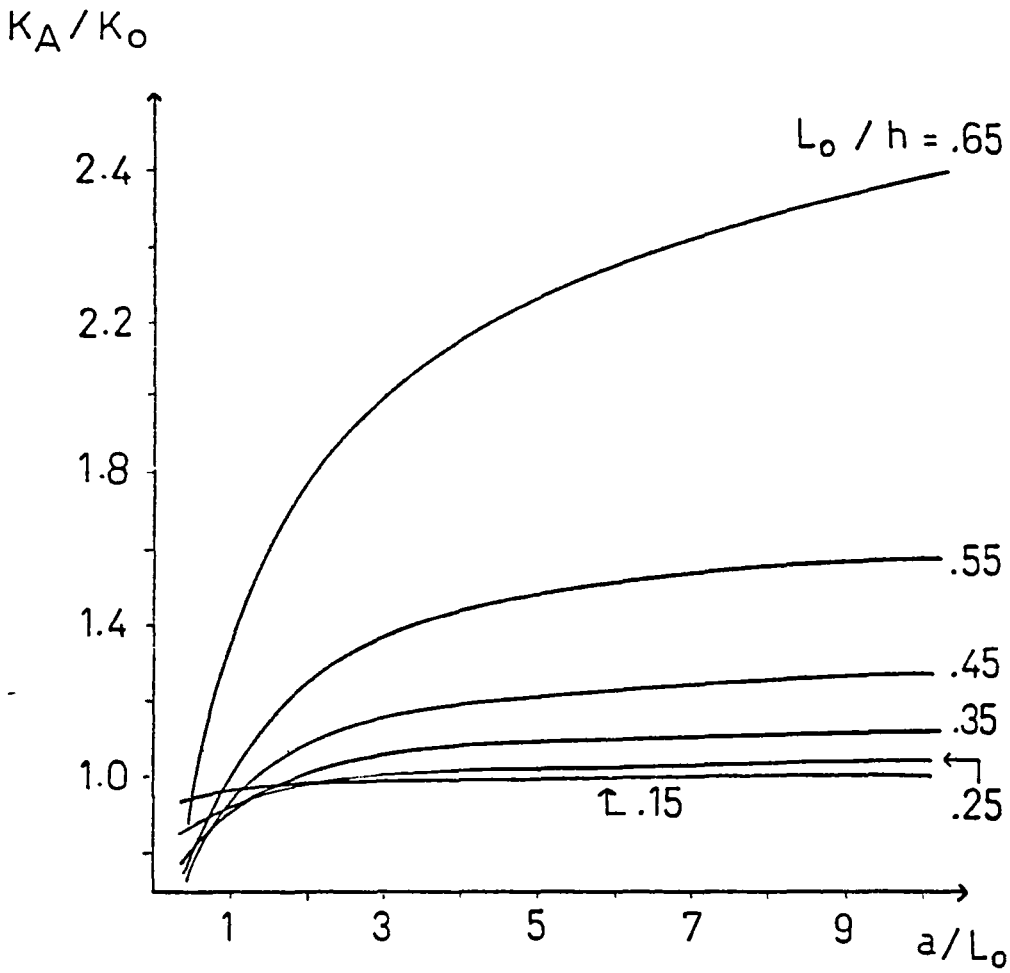

Figure 17. Effect of a/L_o ratio on the normalized stress intensity factors calculated at the midsection of internal elliptic cracks with d/h=0.15 and different L_o/h ratios under pure tension.

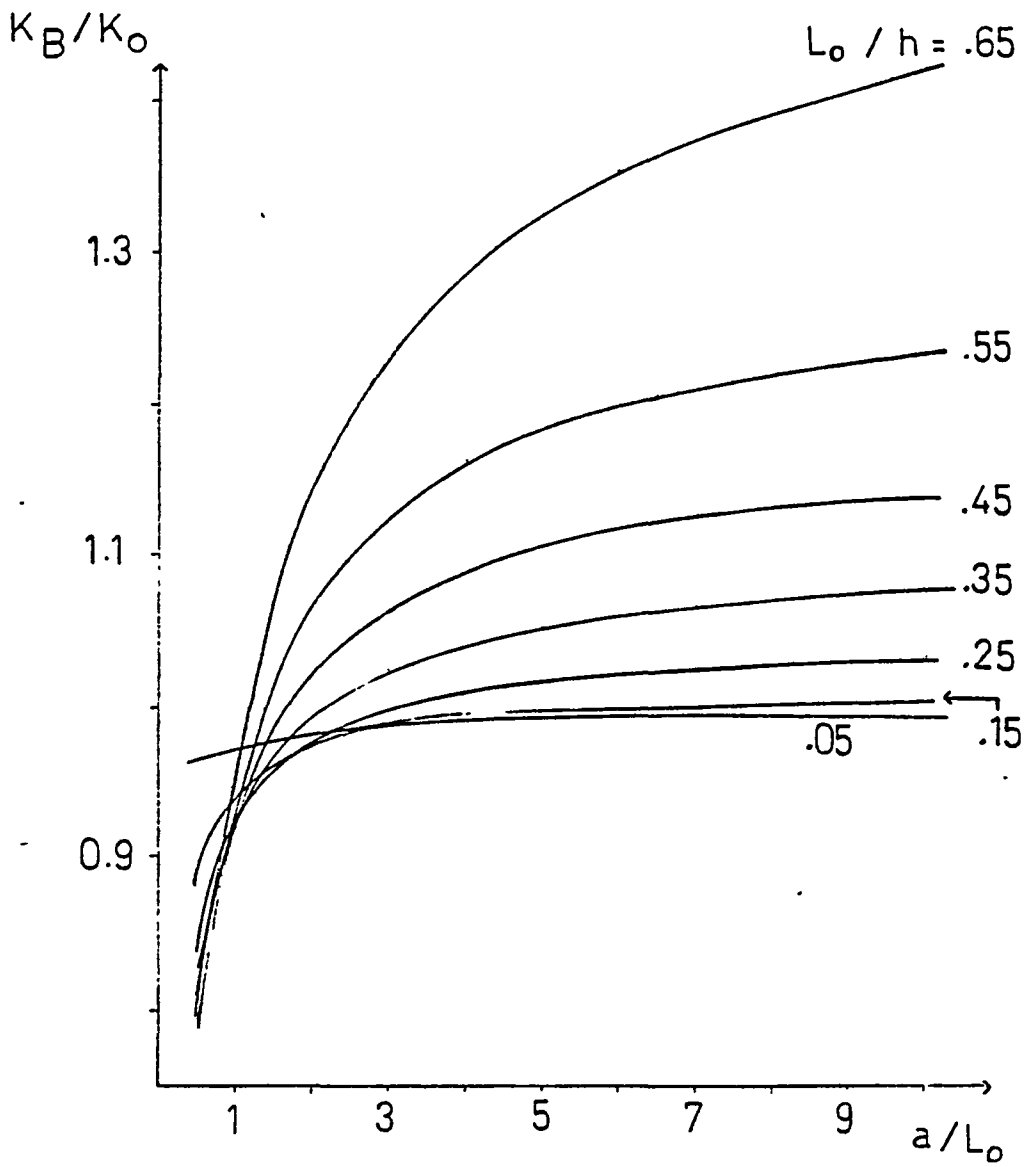

Figure 18. Effect of a/L_o ratio on the normalized stress intensity factors calculated at the midsection of internal elliptic cracks with d/h=0.15 and different L_o/h ratios under pure tension.

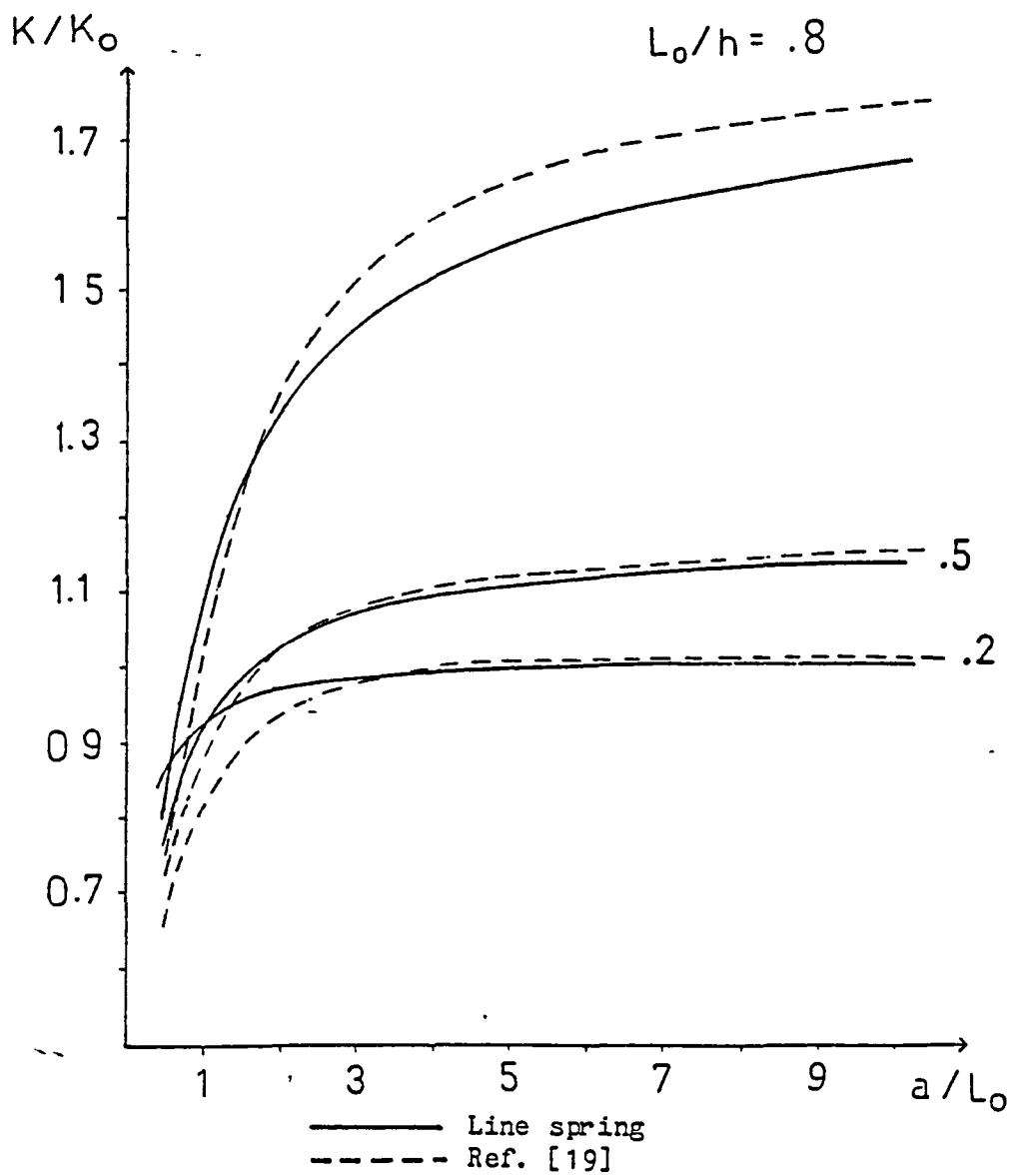

Figure 19. Comparison of the normalized stress intensity factors calculated in this study at x=0 for an internal planar elliptic crack in a plate under uniform tension and with the corresponding values given in Ref.[19].

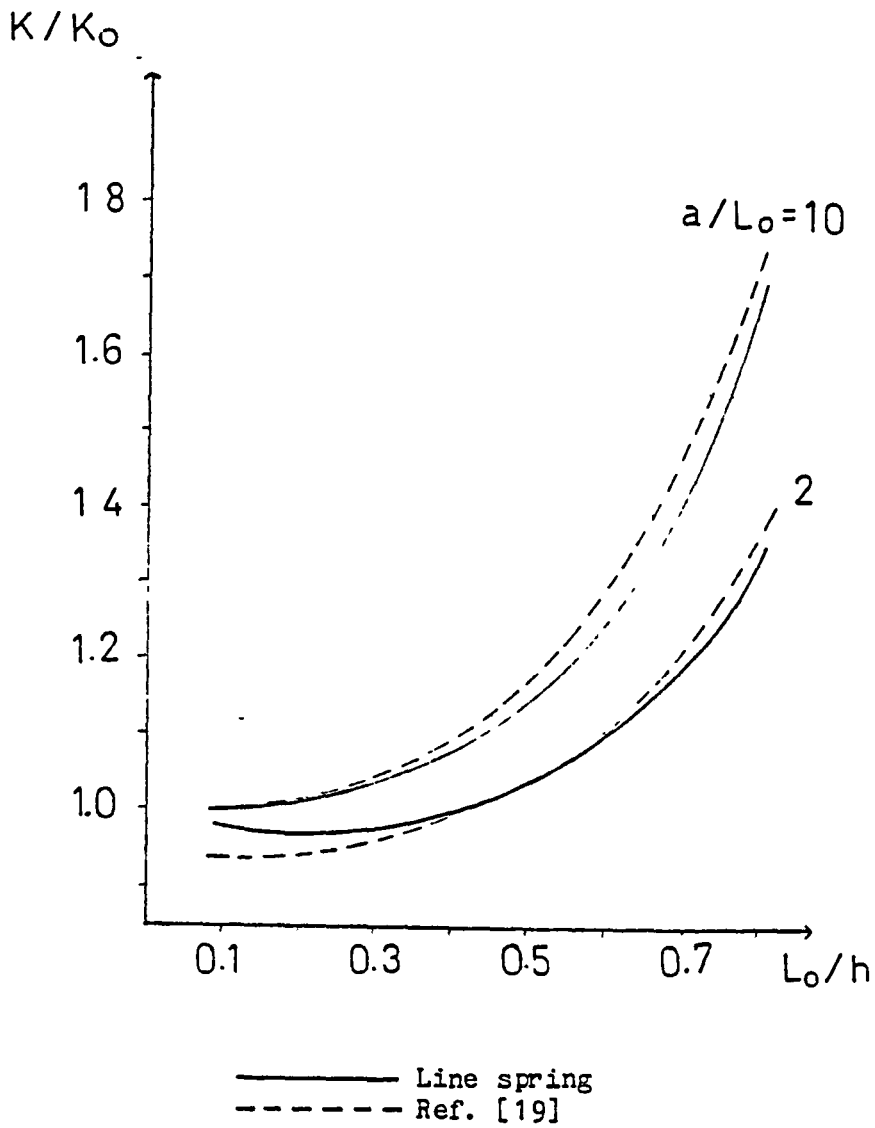

Figure 20. Comparison of the normalized stress intensity factors calculated in this study at x=0 for an internal planar elliptic crack in a plate under uniform tension and with the corresponding values given in Ref.[19].

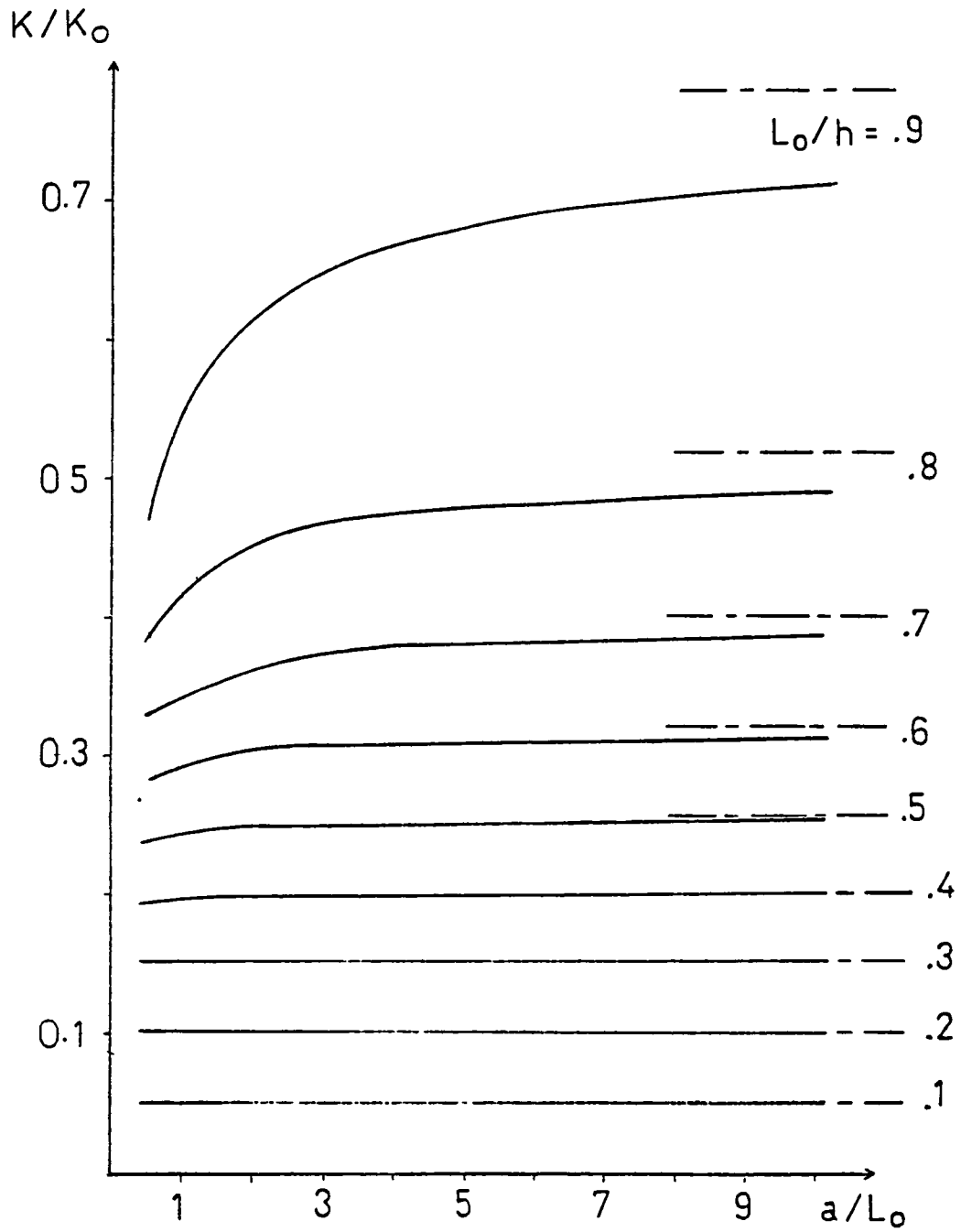

Figure 21. Normalized stress intensity fators calculated at the midsection of a symmetrically located (d/h=0) internal planar elliptic crack in a plate under uniform bending.

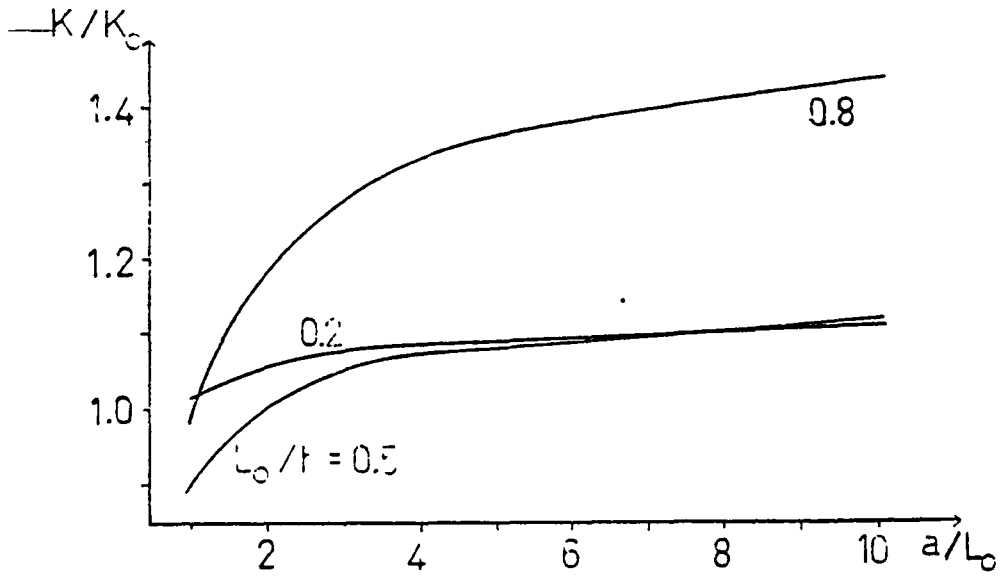

Figure 22. Normalized stress intensity factors calculated at the midsection of two opposite planar elliptic edge cracks in a plate under uniform tension.

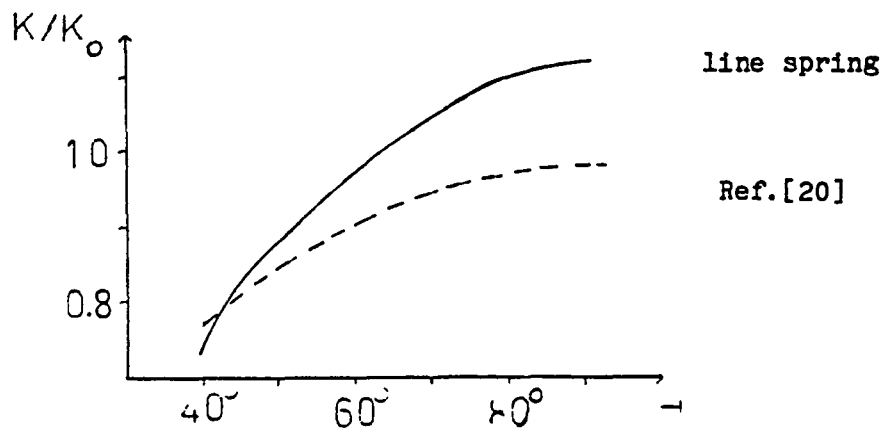

Figure 23. Comparison of the stress intensity factors calculated in this study at the midsection of a symmetrically located internal(d/h=0) planar elliptic crack in a plate under uniform tension with the corresponding results given in [20]. $L_o/h=.57$, $a/L_o=1.25$, $x=\cos\theta$.

REFERENCES

1. F. Delale and F. Erdogan, "Line Spring Model for Surface Cracks in a Reissner Plate", Int. J. Eng. Sci., Vol.19, 1981, pp.1331 .

2. F. Delale and F. Erdogan, "Transverse Shear Effect in a Circumferentially Cracked Cylindrical Shell", Quart. Appl. Math., Vol.37, 1979, pp.239 .

3. J. R. Rice and N. Levy, "The Part-Through Surface Crack in an Elastic Plate", J. of Appl. Mech., Trans. ASME, Vol.39, 1972, pp.185 .

4. F. Erdogan, "Mixed Boundary-Value Problems in Mechanics: Addendum", Mechanics Today, S. Nemat-Nasser(ed), Vol.4, pp.199 .

5. F. W. Smith and D. R. Sorensen, "The Semi-Elliptical Surface Crack - A Solution by the Alternating Method", Int. J. of Fracture, Vol.12, 1976, pp.47 .

6. R. C. Shah and A. S. Kobayashi, "On the Surface Flaw Problem", The Surface Crack: Physical Problems and Computational Solutions, ed. J. L. Swedlow, 1972, pp.79 .

7. J. Heliot, R. C. Labbens, A. Pellisier-Tannon, "Semi Elliptic Cracks in a Cylinder Subjected to Stress Gradients", Fracture Mechanics, ASTM, STP 677, 1979, pp.341 .

8. I. S. Raju, J. C. Newman, Jr., "Stress-Intensity Factors for a Wide Range of Semi-Elliptical Surface Cracks in Finite-Thickness Plates", J. of Eng. Fracture Mechanics, Vol.11, 1979, pp. 817 .

9. J. C. Newman, Jr., "A Review and Assessment of the Stress-Intensity Factors for Surface Cracks", NASA Technical Memorandum 78805, Nov. 1978.

10. S. N. Atluri, K. Kathiresan, A. S. Kobayashi, M. Nakayaki, "Inner Surface Cracks in an Internally Pressurized Cylinder Analyzed by a Three-Dimensional Displacement-Hybrid Finite Element Method", ASME, Part III, New York, 1977, pp.527 .

11. F. Delale and F. Erdogan, "The Effect of Transverse Shear in a Cracked Plate Under Skewsymmetric Loading", J. Appl. Mech., Trans. ASME, Vol.46 .

12. D. M. Parks, "The Inelastic Line Spring: Estimates of Elastic-Plastic Fracture Parameters for Surface Cracked Plates and Shells", ASME, Paper 80-C2/PVP-109, 1980.

13. D. M. Parks, "Inelastic Analysis of Surface Flaws Using the Line Spring Model", Proceedings of the 5'th Int. Conf. on Fracture, Cannes, France, 1981.

14. F. Delale and F. Erdogan, "Application of the Line Spring Model to a Cylindrical Shell Containing a Circumferential or an Axial Part-Through Crack", J. Appl. Mech., Trans. ASME, Vol.49, 1982, pp.97 .

15. F. Erdogan and H. Boduroglu, "Surface Cracks in a Plate of Finite Width Under Extension or Bending", Theoretical and Applied Fracture Mechanics, Vol.1, 1985(to appear).

16. F. Erdogan and O. S. Yahsi, "A Cylindrical Shell With a Stress-Free End Which Contains an Axial Part-Through or Through Crack", Project Report, NASA NGR 39-007-011, Lehigh University, Dec. 1983.

17. F. Erdogan and O. S. Yahsi, "A Pressurized Cylindrical Shell With a Fixed End Which Contains an Axial Part-Through or Through Crack", Project Report, NASA NGR 39-007-011, Lehigh University, Dec. 1983.

18. F. Erdogan and G. D. Gupta, "The Problem of Edge Cracks in an Infinite Strip", J. Appl. Mechanics, Trans. ASME, 1974, pp.1001 .

19. J. C. Newman, Jr. and I. S. Raju, "Stress Intensity Factor Equations for Cracks in Three-Dimensional Finite Bodies", ASTM STP-791, 1983, pp. 238 .

20. T. Nishioka and S. N. Atluri, "Analytical Solution for Embedded Elliptic Cracks, and Finite Element Alternating Method for Elliptical Surface Cracks, Subjected to Arbitrary Loadings", Engineering Fracture Mechanics, Vol.17, 1983, pp.247 .

APPENDIX I

The dimensionless quantities used in the formulation:

$$x = \frac{x_1}{a_i} , \qquad y = \frac{x_2}{a_i} , \qquad z = \frac{x_3}{a_i} ,$$

$$u = \frac{u_1}{a_i} , \qquad v = \frac{u_2}{a_i} , \qquad w = \frac{u_3}{a_i} ,$$

$$\beta_x = \beta_1 , \qquad \beta_y = \beta_2 .$$

$$\lambda^4 = 12 (1 - \nu^2) \frac{a_i^2}{h^2} , \qquad \kappa = \frac{h^2}{5 (1 - \nu) a_i^2} ,$$

$$p = \left[\frac{2}{\kappa(1-\nu)}\right]^{1/2} ,$$

$$R_1 = \frac{a_i(1 - \nu^2)}{2\pi h \lambda^4} , \qquad R_2 = \frac{3 + \nu}{1 + \nu} ,$$

$$R_3 = \frac{4\kappa (1 - \nu)}{(1 + \nu)} , \qquad R_4 = \frac{4}{1 + \nu} .$$

APPENDIX II

Procedure for finding coefficients of the shape functions (g_t and g_b) are as follows. Loading should be seperated as pure tension and pure bending. For pure tension case

$$m = 0 \quad .$$

By using (8), (9) and (10a)

$$K(s) = \sqrt{h}\,\sigma\, g_t(s) \quad ,$$

$$K(s) = \sqrt{h}\,\sigma\,\sqrt{\pi s}\sum_{i=1}^{n} b_i (s)^{2(i-1)} \quad ,$$

$$K(s) = \sigma\sqrt{\pi L(x_1)}\sum_{i=1}^{n} b_i (s)^{2(i-1)} \quad ,$$

$$\frac{K(s)}{\sigma\sqrt{\pi L(x_1)}} = \sum_{i=1}^{n} b_i (s)^{2(i-1)} \quad .$$

Values of the left handside can easily be found for a wide range of s values in related literature, which enables us to create n equations with b_i's as the n unknowns. Solution of this system is the coefficient of corresponding shape function.

Same procedure is followed under pure bending to find c_i's .

APPENDIX III

Solution of the Integral Equations

i- Gauss-Chebyshev Closed Type Integration Formula

The solution of the integral equation which only has the Cauchy type singularity

$$\frac{1}{\pi}\int_{-1}^{1}\frac{\Phi(t)}{t-x}\,dt + \int_{-1}^{1} k(x,t)\,\Phi(t)\,dt = f(x) \quad , \quad -1 < x < 1 \quad ,$$

may be expressed as

$$\Phi(t) = (1 - t^2)^{-1/2} g(t)$$

$$K(x,t) = \frac{1}{\pi}\,\frac{1}{t-x} + k(x,t)$$

$$\frac{\pi}{n-1}\left[\frac{1}{2}K(x_j,t_1)g(t_1) + \sum_{i=2}^{n-1} K(x_j,t_i)g(t_i) + \frac{1}{2}K(x_j,t_n)g(t_n)\right]$$

$$= f(x_j) \quad , \quad j = 1, \ldots\ldots, (n-1)$$

$$t_i = \cos\left[\frac{i-1}{n-1}\pi\right] \quad , \quad i = 1, \ldots\ldots, n$$

$$x_j = \cos\left[\frac{2j-1}{2n-2}\pi\right] , \quad j = 1, \ldots\ldots , (n-1)$$

and the additional condition

$$\int_{-1}^{1} \Phi(t)\, dt = A ,$$

becomes

$$\frac{\pi}{n-1}\left[\frac{1}{2}g(t_1) + \sum_{i=2}^{n-1} g(t_i) + \frac{1}{2}g(t_n)\right] = A$$

One may find the detailed derivation of the formula in [4].

When there is a system of integral equations with more than one unknown functions to be solved, the above procedure can be used by applying the formula to each integration seperately. For example

$$\frac{1}{\pi}\int_{-1}^{1}\frac{\Phi_1(t)}{t-x}\,dt + \int_{-1}^{1} k_{11}(x,t)\Phi_1(t)\,dt + \int_{-1}^{1} k_{12}(x,t)\Phi_2(t)\,dt = f_1(x) ,$$

$$\int_{-1}^{1} k_{21}(x,t)\Phi_1(t)\,dt + \int_{-1}^{1} k_{22}(x,t)\Phi_2(t)\,dt + \frac{1}{\pi}\int_{-1}^{1}\frac{\Phi_2(t)}{t-x}\,dt = f_2(x) ,$$

$$\int_{-1}^{1} \Phi_1(t)\, dt = A_1 , \qquad \int_{-1}^{1} \Phi_2(t)\, dt = A_2 , \qquad -1 < x < 1$$

can be solved as

$$\Phi_1(t) = (1 - t^2)^{-1/2} g_1(t) ,$$

$$\Phi_2(s) = (1 - s^2)^{-1/2} g_2(s) ,$$

s has been introduced to define different collocation points for each functions.

$$K_{11}(x,t) = \frac{1}{\pi} \frac{1}{t-x} + k_{11}(x,t) ,$$

$$K_{12}(x,s) = k_{12}(x,s) ,$$

$$K_{21}(x,s) = k_{21}(x,s) ,$$

$$K_{22}(x,s) = \frac{1}{\pi} \frac{1}{s-x} + k_{22}(x,s) ,$$

$$\frac{\pi}{n_1-1}\left[\frac{1}{2}K_{11}(x_j,t_1)g_1(t_1)+\sum_{i=2}^{n_1-1}K_{11}(x_j,t_i)g_1(t_i)+\frac{1}{2}K_{11}(x_j,t_{n1})g_1(t_{n1})\right]$$

$$+\frac{\pi}{n_2-1}\left[\frac{1}{2}K_{12}(x_j,s_1)g_2(s_1)+\sum_{i=2}^{n_2-1}K_{12}(x_j,s_i)g_2(s_i)\right.$$

$$\left.+\frac{1}{2}K_{12}(x_j,s_{n2})g_2(s_{n2})\right]=f_2(x_j)\ ,$$

$$x_j=\cos\left[\frac{2j-1}{2n_1-2}\pi\right]\ ,\qquad j=1,\ .....\ ,(n_1-1)$$

$$\frac{\pi}{n_1-1}\left[\frac{1}{2}K_{21}(x_j,t_1)g_1(t_1)+\sum_{i=2}^{n_1-1}K_{21}(x_j,t_i)g_1(t_i)+\frac{1}{2}K_{21}(x_j,t_{n1})g_1(t_{n1})\right]$$

$$+\frac{\pi}{n_2-1}\left[\frac{1}{2}K_{22}(x_j,s_1)g_2(s_1)+\sum_{i=2}^{n_2-1}K_{22}(x_j,s_i)g_2(s_i)\right.$$

$$\left.+\frac{1}{2}K_{22}(x_j,s_{n2})g_2(s_{n2})\right]=f_2(x_j)$$

$$X_j=\cos\left[\frac{2j-1}{2n_2-2}\pi\right]\ ,\qquad j=1,\ .....\ ,(n_2-1)$$

$$\frac{\pi}{n_1-1}\left[\frac{1}{2}g_1(t_1)+\sum_{i=2}^{n_1-1}g_1(t_i)+\frac{1}{2}g_1(t_{n1})\right]=A_1\ ,$$

$$\frac{\pi}{n_2-1}\left[\frac{1}{2}g_2(s_1)+\sum_{i=2}^{n_2-1}g_2(s_i)+\frac{1}{2}g_2(s_{n2})\right]=A_2\ ,$$

$$t_i = \cos\left[\frac{i-1}{n_1-1}\pi\right], \qquad i = 1, \ldots\ldots, n_1$$

$$s_i = \cos\left[\frac{i-1}{n_2-1}\pi\right], \qquad i = 1, \ldots\ldots, n_2$$

Above solution can also be used for any number of unknown functions in the same manner.

ii- Order of Singularity in the Integral Equation

At first glance, it seems that (31) has singularities other than Cauchy type. But if we take a closer look to the equation, we will see that modified Bessel function of the second kind has the following property for relatively small values of the argument.

$$K_r(x) \sim 2^{r-1}(r-1)!x^{-r} \quad ,$$

$$K_2(x) \sim 2\,x^{-2} \quad .$$

By using above property, we can say that

$$\lim_{(t-x)\to 0} K_2(p|t-x|) = \frac{2}{p^2(t-x)^2} = \frac{K(1-p)}{(t-x)^2}$$

which gives

$$\lim_{(t-x)\to 0} \left[\frac{4}{1+\nu} \frac{1}{t-x} K_2(p|t-x|) - \frac{4\kappa(1-\nu)}{1+\nu} \frac{1}{(t-x)^3} \right] = 0 \quad .$$

This proves that (31) has only Cauchy type singularity and can be solved by Gauss-Chebyshev closed type integration formula.

Integrals on the interval (-1 , x) can be written on (-1 , +1) by redifining the kernels by the use of a step function H(y) as follows:

$$\int_{-1}^{x} f(t)\, dt = \int_{-1}^{1} H(x-t)\, f(t)\, dt$$

where,

$$H(y) = \begin{cases} 0 & \text{if} \quad y < 0 \\ 1 & \text{if} \quad y \geq 0 \ . \end{cases}$$

APPENDIX IV

Numerical Integration

Gauss-Chebyshev closed type integration formula is used for numerical integration purposes. Any integral in the interval (-1 , +1) can be expressed as,

$$\int_{-1}^{1} \frac{f(x)\,dx}{\sqrt{1-x^2}} = \frac{\pi}{n-1}\left[\frac{1}{2} f(x_1) + \sum_{i=2}^{n-1} f(x_i) + \frac{1}{2} f(x_n)\right]$$

If an integration in the interval (-1 , x) is desired, above formula can again be used by multiplying the integrand with the H function defined in Appendix III.

Number of points (n) in the integration should be much higher than the number of points used in the solution of integral equations if one desires to evaluate the stress intensity factor or the crack front at any point accurately. Values of the functions to be integrated at any point can be found by interpolating the function between the two surrounding known values found from the solution of integral equations.

1 Report No	2 Government Accession No	3 Recipient's Catalog No
NASA CR-177926		

4 Title and Subtitle	5 Report Date
Interaction of Part-Through Cracks in a Flat Plate	April 1985
	6 Performing Organization Code
7 Author(s)	8 Performing Organization Report No
B. Aksel and F. Erdogan	
	10 Work Unit No
9 Performing Organization Name and Address	11 Contract or Grant No
Lehigh University Department of Mechanical Engineering Bethlehem, PA	NGR 39-007-011
	13 Type of Report and Period Covered
12 Sponsoring Agency Name and Address	Contractor Report
National Aeronautics and Space Administration Washington, DC 20546	14 Sponsoring Agency Code 505-33-23-02

15 Supplementary Notes

Langley Technical Monitor: W. Steven Johnson

16 Abstract

Main purpose of this study is to determine the accuracy of the line spring model, to investigate the effect of interaction between two and three cracks, and to provide extensive numerical results which may be useful in applications. Line spring model with Reissner's plate theory is formulated to be used for any number and configurations of cracks provided that there is symmetry. This model is used to find stress intensity factors for elliptic internal cracks, elliptic edge cracks and two opposite elliptic edge cracks. Unfortunately, because of the unavailability of previous work done on the cases considered, only stress intensity factors for central elliptic crack could be compared with other methods. Despite the simplicity of the line spring model, the results are found to be surprisingly close.

17 Key Words (Suggested by Author(s))	18 Distribution Statement
line spring model, cracks, Reissner's plate theory, stress intensity factors	Unclassified - Unlimited Subject Category 39

19 Security Classif (of this report)	20 Security Classif (of this page)	21. No of Pages	22 Price*
Unclassified	Unclassified	113	A06

*For sale by the National Technical Information Service, Springfield, Virginia 22151

End of Document